Agricultural and Forest Meteorology 151 (2011) 22–38

Contents lists available at ScienceDirect

Agricultural and Forest Meteorology

journal homepage: www.elsevier.com/locate/agrformet

Assessing parameter variability in a photosynthesis model within and between plant functional types using global Fluxnet eddy covariance data

M. Groenendijk[a,*], A.J. Dolman[a], M.K. van der Molen[a], R. Leuning[b], A. Arneth[c], N. Delpierre[d], J.H.C. Gash[a,e], A. Lindroth[c], A.D. Richardson[f], H. Verbeeck[g], G. Wohlfahrt[h]

[a] VU University Amsterdam, Hydrology and Geo-Environmental Sciences, The Netherlands
[b] CSIRO Marine and Atmospheric Research, Canberra, Australia
[c] Department of Earth and Ecosystem Sciences, Lund University, Sweden
[d] Universite Paris-Sud, Laboratoire Ecologie Systematique et Evolution, UMR8079, Orsay F-91405, France
[e] Centre for Ecology and Hydrology, Wallingford, UK
[f] Harvard University, Department of Organismic and Evolutionary Biology, HUH, 22 Divinity Avenue, Cambridge, MA 02138, USA
[g] Laboratory of Plant Ecology, Ghent University, Coupure Links 653, 9000 Ghent, Belgium
[h] Institut für Ökologie, Universität Innsbruck, Austria

ARTICLE INFO

Article history:
Received 14 July 2010
Received in revised form 27 August 2010
Accepted 31 August 2010

Keywords:
Plant functional types
Model parameters
Photosynthesis
Transpiration
Eddy covariance
Fluxnet

ABSTRACT

The vegetation component in climate models has advanced since the late 1960s from a uniform prescription of surface parameters to plant functional types (PFTs). PFTs are used in global land-surface models to provide parameter values for every model grid cell. With a simple photosynthesis model we derive parameters for all site years within the Fluxnet eddy covariance data set. We compare the model parameters within and between PFTs and statistically group the sites. Fluxnet data is used to validate the photosynthesis model parameter variation within a PFT classification.

Our major result is that model parameters appear more variable than assumed in PFTs. Simulated fluxes are of higher quality when model parameters of individual sites or site years are used. A simplification with less variation in model parameters results in poorer simulations. This indicates that a PFT classification introduces uncertainty in the variation of the photosynthesis and transpiration fluxes. Statistically derived groups of sites with comparable model parameters do not share common vegetation types or climates.

A simple PFT classification does not reflect the real photosynthesis and transpiration variation. Although site year parameters give the best predictions, the parameters are generally too specific to be used in a global study. The site year parameters can be further used to explore the possibilities of alternative classification schemes.

© 2010 Elsevier B.V. All rights reserved.

1. Introduction

The specification of the land surface component of climate models has evolved through four major steps over the past four decades. The first generation in the late 1960s had a uniform prescription of surface parameters (see reviews by Sellers et al., 1997; Pitman, 2003), while the second generation in the 1980s introduced the concept of plant functional types (PFTs) to describe the effects of spatially varying vegetation on the surface energy balance (e.g. Sellers et al., 1986; Dickinson et al., 1986). In the third generation of models vegetation is simulated dynamically rather than being prescribed (Friend and Cox, 1995; Sellers et al., 1997; Foley et al., 1998; Woodward et al., 1998; Cox et al., 2000), while the latest models couple vegetation dynamics to the carbon and nitrogen cycles (Thornton et al., 2009; Yang et al., 2009; Zaehle and Friend, 2010), and include processes for emissions of reactive trace gases, vegetation–fire interactions and crop–biogeochemistry interactions (Arneth et al., 2010).

To run these land-surface models globally, it is necessary to provide parameter values for every model grid cell, and typically this is done by assigning a unique parameter set for each PFT. Early PFT classifications were developed for calculating the surface energy and water balance and were largely based on broad classes of vegetation. Later these PFTs were applied to deduce the carbon balance of the land surface, even though a number of carbon cycle processes might not run parallel to the energy and water processes upon which the original classifications were based. More recently PFT classifications have been derived following either a deductive or an inductive approach (Woodward and Cramer, 1996). Examples of PFT classifications derived using the deductive approach are

* Corresponding author.
E-mail address: margriet.groenendijk@falw.vu.nl (M. Groenendijk).

0168-1923/$ – see front matter © 2010 Elsevier B.V. All rights reserved.
doi:10.1016/j.agrformet.2010.08.013

presented by Box (1996), Bonan et al. (2002) and Sitch et al. (2003). Here the criteria for PFTs are based on climatic limitations such as temperature, precipitation and length of the growing season. These PFTs are subjectively classified based on a general understanding of processes. With the inductive approach (Woodward and Cramer, 1996) PFTs are derived from sets of observations or experimental results e.g. through statistical clustering with climatic variables and vegetation traits (Chapin et al., 1996; Wang and Price, 2007).

The assumption that parameters in carbon exchange models can conveniently be allocated to PFTs appears to contradict observed gradual transitions between different ecosystem types. Kleidon et al. (2007) show that the strict separation of vegetation into less than eight PFTs may lead to artificial multiple steady-states in a model of the Earth's climate–vegetation system depending on the number of PFTs used. Measurements on individual leaves indicate a gradual transition in vegetation characteristics. Leaf traits are inter-related e.g., maximum photosynthetic capacity, maintenance respiration, nitrogen concentration, leaf life span and specific leaf area (ratio of leaf surface area to leaf mass) (Reich et al., 1997; Bonan et al., 2002; Meinzer, 2003; Wright et al., 2004). Harrison et al. (2010) therefore suggest using these continuous traits for the development of a new vegetation classification.

On the global scale it is a challenging task to provide sufficient data for a complete PFT classification, because a large number of observations are needed for each PFT (Wang and Price, 2007). Many studies have used eddy covariance data from Fluxnet (a global network of sites), showing the variation in carbon and water fluxes between vegetation types and along climate gradients (e.g., Baldocchi, 2008; Law et al., 2002; Friend et al., 2007; Luyssaert et al., 2007; Stöckli et al., 2008; Stoy et al., 2009; Beer et al., 2009; Yuan et al., 2009; Williams et al., 2009). The eddy covariance data can also be used to derive model parameters (e.g., Reichstein et al., 2003b; van Dijk and Dolman, 2004; Knorr and Kattge, 2005; Raupach et al., 2005; Owen et al., 2007; Richardson et al., 2007; Wang et al., 2007; Thum et al., 2008). However, hardly any of these studies have attempted to derive model parameters for key carbon cycle processes such as photosynthesis for the full set of data.

This study uses a simple vegetation model to derive the parameters for all site years and vegetation types within the Fluxnet database. We compare the set of model parameters within and between PFTs and group the sites statistically. We combine the deductive and inductive PFT classifications to give insight into the variation of model parameters. We address the following specific questions: (1) what is the variability of parameter values for a set of conventionally defined PFTs, (2) how well are fluxes simulated using parameter values for each PFT compared to using site-calibrated values at diurnal, seasonal and annual time scales, (3) if using mean or median values provides unsatisfactory results, is it sufficient to refine the classification scheme and, (4) if this is unsatisfactory, does a cluster analysis of parameters provide a satisfactory solution?

2. Methodology

2.1. Model description

The photosynthesis model of Farquhar et al. (1980) is widely used in vegetation models (e.g., Sellers et al., 1996; Arora, 2002; Sitch et al., 2003; Krinner et al., 2005; Rayner et al., 2005). Individual applications of this model differ in the influence they ascribe to environmental factors, the scaling from leaf to ecosystem and the way how the model is assigned to different PFTs. The simple vegetation model used in this study is based on the equations derived by Cowan (1977) and Farquhar et al. (1980). The model includes responses of photosynthesis and transpiration to air temperature, photosynthetically active radiation, vapor pressure deficit and soil water content. The model parameters are assumed to represent the relationship between nutrients and vegetation characteristics, and the adaptation to local climatic conditions.

Table 1
Parameters used in the photosynthesis and transpiration model. Values given are the default or initial* values within the model optimization.

Parameter	Description	Value
$v_{cm,25}$	Carboxylation capacity (μmol m^{-2} s^{-1})	100*
$j_{m,25}$	Electron transport rate, (μmol m^{-2} s^{-1})	300*
α	Quantum yield (mol mol^{-1})	0.7*
λ	Water use efficiency (mol mol^{-1})	8000*
O	O_2 concentration (mbar)	210
T_{ref}	Reference temperature for photosynthesis (K)	298.15
$K_{c,25}$	Kinetic coefficient for CO_2 at T_{ref} (μbar)	460
$K_{o,25}$	Kinetic coefficient for O_2 at T_{ref} (mbar)	330
E_{kc}	Activation energy for CO_2 (J mol^{-1})	59,356
E_{ko}	Activation energy for O_2 (J mol^{-1})	35,948
E_{jm}	Activation energy for j_m (J mol^{-1})	45,000
E_{vcm}	Activation energy for v_{cm} (J mol^{-1})	58,520

The main parameters in this model are $v_{cm,25}$, $j_{m,25}$, α and λ (Table 1). $v_{cm,25}$ is the rate of carboxylation mediated by the enzyme Rubisco, $j_{m,25}$ is the maximum potential electron transport rate and α is the quantum yield. λ defines the ratio between water loss (transpiration) and CO_2 assimilation (photosynthesis) as a function of stomatal conductance (g_s) as proposed in the optimality hypothesis which states that plants optimize their stomatal conductance to maximize photosynthesis for a given amount of transpiration (Cowan, 1977):

$$\lambda = \frac{\delta E/\delta g_s}{\delta A/\delta g_s} \tag{1}$$

This stomatal conductance model was successfully used to reproduce observed ecosystem carbon and water fluxes by Arneth et al. (2002, 2006), van der Tol et al. (2007, 2008), Mercado et al. (2009) and Schymanski et al. (2009). Schymanski et al. (2007) compared the use of this model with the stomatal conductance model of Leuning (1995) and concluded that both models performed equally well in reproducing observed transpiration rates. A complete model description with scaling from the leaf to the ecosystem scale and temperature responses is presented in Appendix A.

2.2. Observations

The Fluxnet database contains fluxes measured with the eddy covariance technique (Aubinet et al., 2000) at more than 200 locations worldwide. All data is processed in a harmonized manner within the Fluxnet project (Baldocchi et al., 2001; Baldocchi, 2008) as described by Papale et al. (2006), Reichstein et al. (2005), Moffat et al. (2007) and Papale and Valentini (2003). The data used here were retrieved from the database in April 2008.[1] A complete list of the sites used is given in Appendix B; Table 2 lists the PFTs used. These sites were selected based on data availability. To apply the model for photosynthesis (A) and transpiration (E) fluxes requires the following variables: Net Ecosystem Exchange (NEE), Latent Heat Flux (LE), vapor pressure deficit (VPD), air temperature (T_a), global radiation (R_g), leaf area index (LAI) and soil water content (θ). Sites with data gaps of more than 50% during the growing season or missing input variables were excluded from the analysis. The 101 selected sites contain 453 site years of which 349 years contain sufficient observations (not gap-filled) to simulate the fluxes. For 57 site years there were no LAI data available, mainly because there

[1] www.fluxdata.org, dataset DS2.

Table 2
Number of Fluxnet sites used in this study within plant functional types as classes of vegetation and climate.

	Arctic	Boreal	Subtropical Mediterranean	Temperate	Temperate continental	Tropical	Total
Cropland			2	3			5
Closed shrubland			1				1
Deciduous broadleaf forest		2	6	6	4		18
Evergreen broadleaf forest			2	1		4	7
Evergreen needleleaf forest		17	9	10	4		40
Grassland	1		3	13			17
Mixed Forest			2	2	3		7
Open shrubland		1			1		2
Savanna			1			1	2
Wetland				1			1
Woody Savanna						1	1
Total	1	20	27	36	11	6	101

were no remotely sensed observations before 2000, and for 57 (different) site years soil water content data was unavailable.

LAI is derived from the MODIS database and is used as a proxy for phenology (ORNL DAAC, 2009). This database contains 8-day composite values of LAI for each site based on 7 km × 7 km data sets centered around the sites. From these pixels the average is calculated from observations with no clouds and no presence of snow or ice. The 8-day composites are linearly interpolated to determine daily values.

The observed carbon flux from eddy covariance represents the net exchange of carbon between ecosystem and atmosphere. The observed flux (F_c) plus a term representing storage within the vegetation is assumed to be equal to *NEE*. Nighttime *NEE* is assumed to be equal to ecosystem respiration (R_e). Within the Fluxnet database the observed *NEE* is partitioned into gross primary production (*GPP*) and R_e. R_e is determined from a temperature function of nighttime fluxes by using the methodology of Reichstein et al. (2005). In our study this *GPP* or photosynthesis flux is used.

The model requires the knowledge of the transpiration flux to estimate model parameters, whereas the observed water vapor flux (*LE*) is the sum of transpiration and soil evaporation. However, the latter contributes little to total evaporation when the soil surface is dry, or when $LAI > 2.5$, because then little energy is available for evaporation. It was thus assumed that total evaporation equals transpiration when the vegetation is dry, and these periods were selected by excluding data during days with precipitation and 3 days thereafter. Using data for several sites showed that estimates of model parameters remained constant with removal of data after rainfall for 3 or more days.

2.3. Model parameter estimation

The model is optimized using the simplex search method (Lagarias et al., 1998). A least squares objective function, or normalized root mean square error is minimized to give the optimal model parameters. This is a multi-criteria problem with both photosynthesis and transpiration being parameterized, therefore the objective function consists of two parts. The normalized root mean square errors ($RMSE_n$) derived from half-hourly observations of the two fluxes are added, giving equal weight to both processes:

$$RMSE_n = \frac{\sqrt{(\sum (A_{sim} - A_{obs})^2)/N}}{\overline{A_{obs}}} + \frac{\sqrt{(\sum (E_{sim} - E_{obs})^2)/N}}{\overline{E_{obs}}} \quad (2)$$

where A_{sim} is simulated photosynthesis, A_{obs} daytime *GPP*, E_{sim} simulated transpiration and E_{obs} observed transpiration. The model parameters were derived for all sites within the Fluxnet database or for different groups of site years classified by vegetation type and climate.

2.4. Grouping sites based on model parameters

The deductive classification is based on an understanding of processes that determine the functioning of vegetation (Woodward and Cramer, 1996). One example is the classical grouping of sites into vegetation classes (Table 2). Inductive classification groups are directly derived from sets of observations. This approach can be applied with statistical clustering. Here we use the model parameters to group the sites. This is a combination of the two classifications, because derived parameters and not the direct observations are used to classify the sites.

Two statistical methods are used and compared, hierarchical and *k*-means clustering. Hierarchical clustering groups data by creating a cluster tree or dendrogram. The tree is a multilevel hierarchy, where clusters at one level are joined to clusters at the next level. *k*-means clustering partitions *n* observations into *k* clusters. Parameter values within each cluster are as close to each other as possible, but as far as possible from values in other clusters. The centre of each cluster is the point to which the sum of distances from all values in that cluster is minimized. The result is a set of clusters that are as compact and well-separated as possible (Seber, 1984). The MATLAB software package was used for both the optimization of the model and the analysis of the results.

3. Results

3.1. Evaluation of flux simulations

Half-hourly observations of fluxes and environmental variables were used to optimize the model with annual parameters. Five sets of parameters were derived: for all sites together (A), for groups of sites with a similar vegetation type (V), for groups of sites with a similar vegetation type and climate (VC), for individual sites (S) and for individual site years (SY). The quality of the simulations for these five parameter sets is presented for the diurnal, seasonal and annual time scales.

The average diurnal cycle in July derived from observations of photosynthesis (*A*) and transpiration (*E*) is compared with fluxes simulated with vegetation model parameters (V, Fig. 1) and fluxes simulated with model parameters of individual site years (SY, Fig. 2). Examples are presented for a tropical evergreen broadleaf forest in Brazil, a boreal evergreen needleleaf forest in Finland and a subtropical grassland in the US. The diurnal variation for these different locations is captured best with simulations that use site year parameters. When using vegetation parameters the fluxes are over- or underestimated (BR-Ban and FI-Hyy) or photosynthesis and transpiration start too late in the morning (US-Goo).

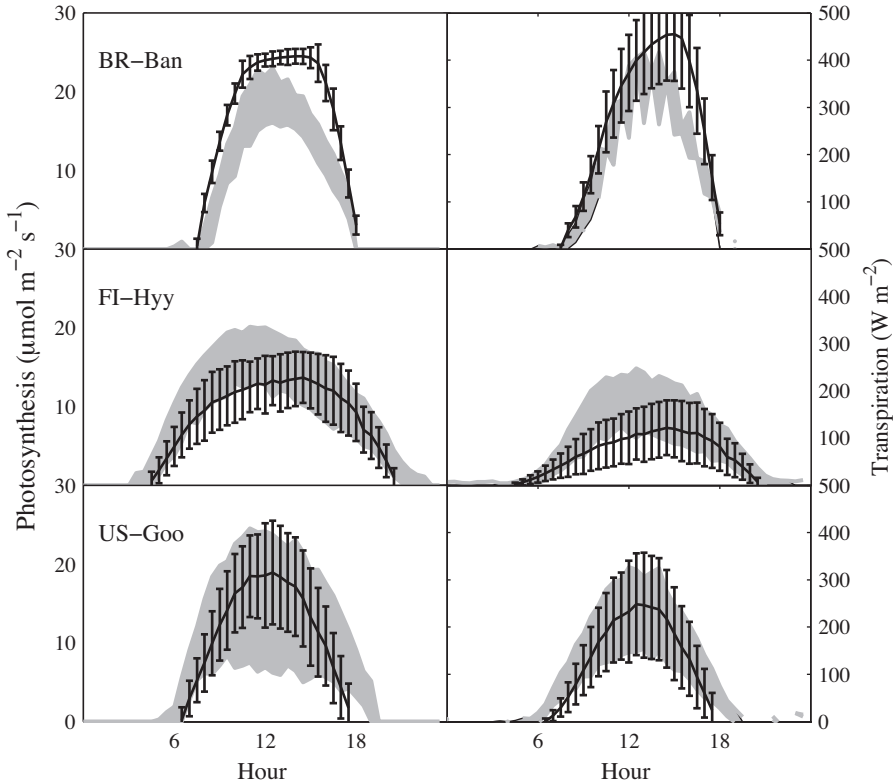

Fig. 1. Comparison of the observed and simulated average diurnal cycle of photosynthesis (left) and transpiration (right) in July for three different sites. The fluxes are simulated with parameters derived for all sites with a similar vegetation type (V, Table 3). The average observed fluxes with standard deviations are presented by the grey area and the average simulated fluxes with standard deviations by the black lines.

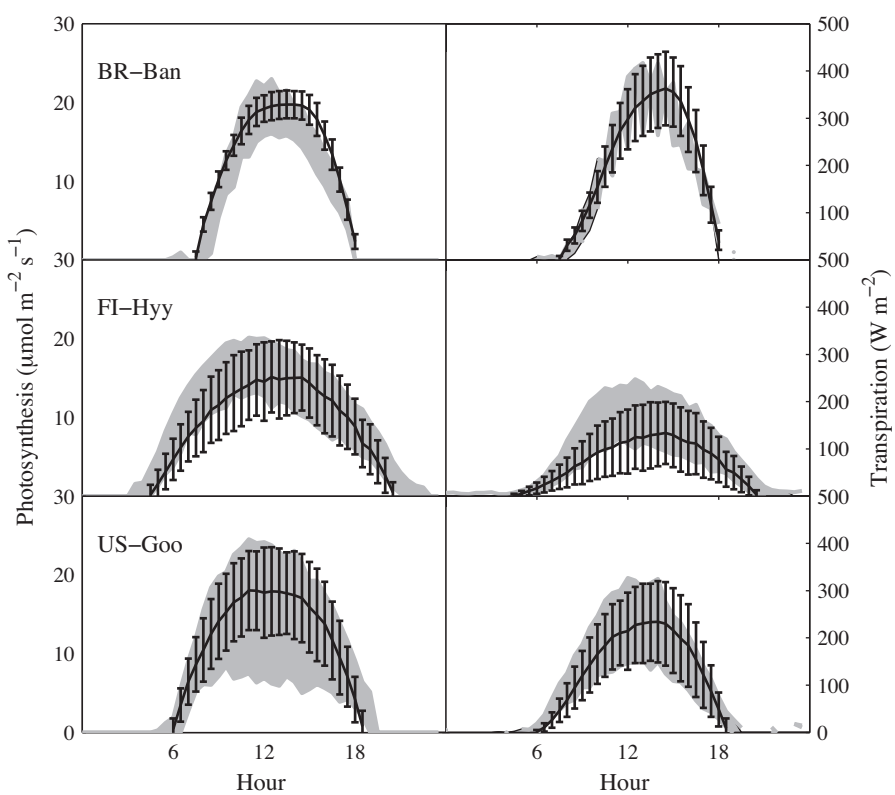

Fig. 2. Comparison of the observed and simulated average diurnal cycle of photosynthesis (left) and transpiration (right) in July for three different sites. The fluxes are simulated with parameters derived for each site year (SY). The average observed fluxes with standard deviations are presented by the grey area and the average simulated fluxes with standard deviations by the black lines.

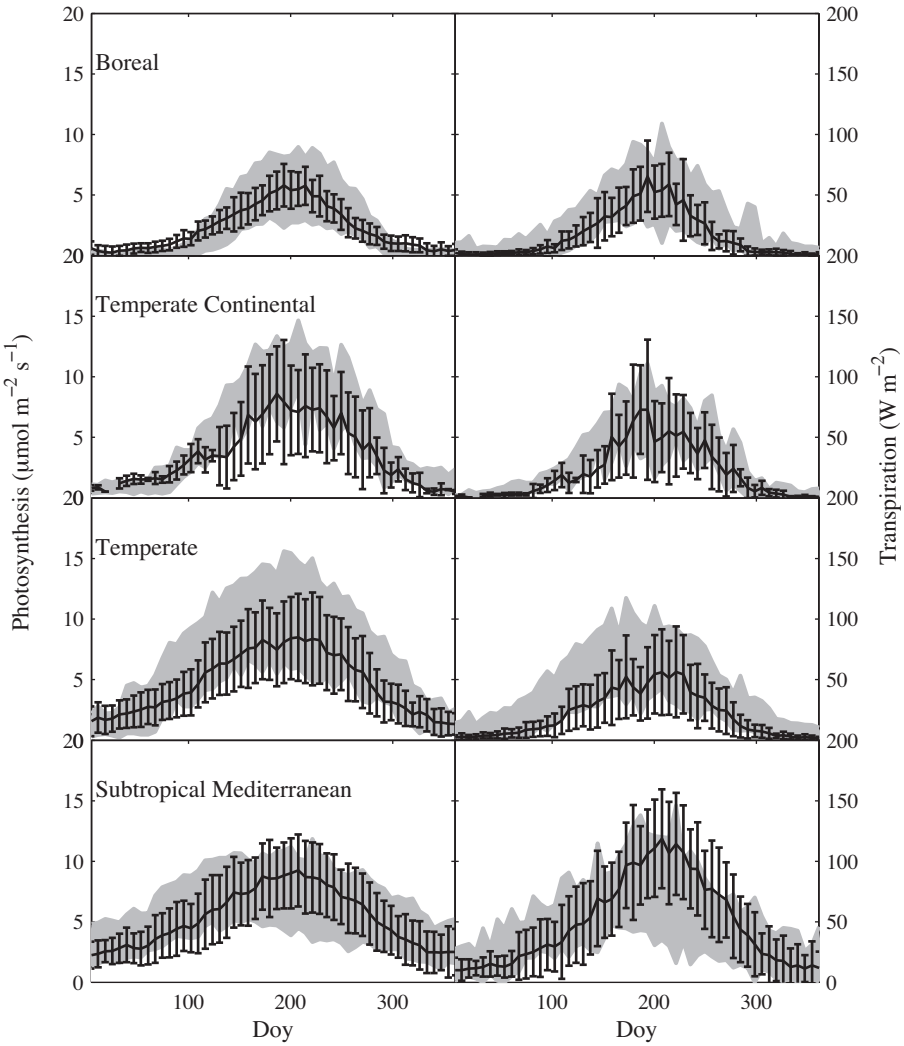

Fig. 3. Seasonal variation of the average weekly observed and simulated photosynthesis (left) and transpiration (right) for the evergreen needle leaf forest sites in four different climates. The fluxes are simulated with parameters derived for all sites with a similar vegetation type and climate (VC, Table 4). The average observed fluxes with standard deviations are presented by the grey area and the average simulated fluxes with standard deviations by the black lines.

Observed and simulated average seasonal cycles of A and E and their standard deviations are shown in Figs. 3 and 4 for evergreen needleleaf forest (ENF) sites growing in four climatic zones. A comparison is made between fluxes simulated with PFT model parameters as in Table 4 (VC) and fluxes simulated with model parameters of individual site years (SY). The average seasonal cycle of simulated A and E of boreal ENF sites is comparable to the observations in both figures. Standard deviations are only correct when using the site year parameters, fluxes simulated with PFT parameters show too little variation. For temperate continental and temperate ENF sites fluxes simulated with PFT parameters are underestimated, while the simulations using site year parameters show a seasonal variation, which is closer to the observations. In the subtropical and Mediterranean regions the fluxes are overestimated in both figures, particularly during summer.

Annual simulated fluxes are compared with observations in Fig. 5. The coefficients of determination (r^2) for annual A and E range from 0.39 to 0.93. The deviation between observations and simulations increases when using more general model parameters, which are derived for larger groups of sites. Simulations using vegetation parameters (V) or PFT parameters (VC) instead of one single parameter set (A) show only very minor improvements. Simulated fluxes are of a higher quality only when model parameters of individual sites (S) or site years (SY) are used. A simplification with less variation in model parameter values results evidently in poorer simulations with deviations of both the diurnal and seasonal cycles resulting in over- or underestimation of annual fluxes.

3.2. Model parameter variation within and across vegetation types

Fig. 6 shows that the mean parameter values and their standard deviations can differ considerably for each vegetation type depending on how the data are classified. For example, the mean values of $v_{cm,25}$ and λ systematically increase for cropland, savanna and evergreen needleleaf forest vegetation types as the data are segregated according to vegetation type (V), vegetation and climate (VC), sites (S) or site-years (SY). While it is difficult to discern systematic trends in other parameters and for other vegetation classes, the different classifications do not strongly affect the relative ranking of parameter values, e.g. the highest values of $v_{cm,25}$ are for croplands and the highest λ for savannas. For each vegetation type in Fig. 6 an average of different parameter sets is presented. The vegetation parameters (V) are derived for all sites within a group, and therefore do not have a standard deviation. The PFT parameters (VC) are derived with climates within a vegetation type as in Table 4, the site

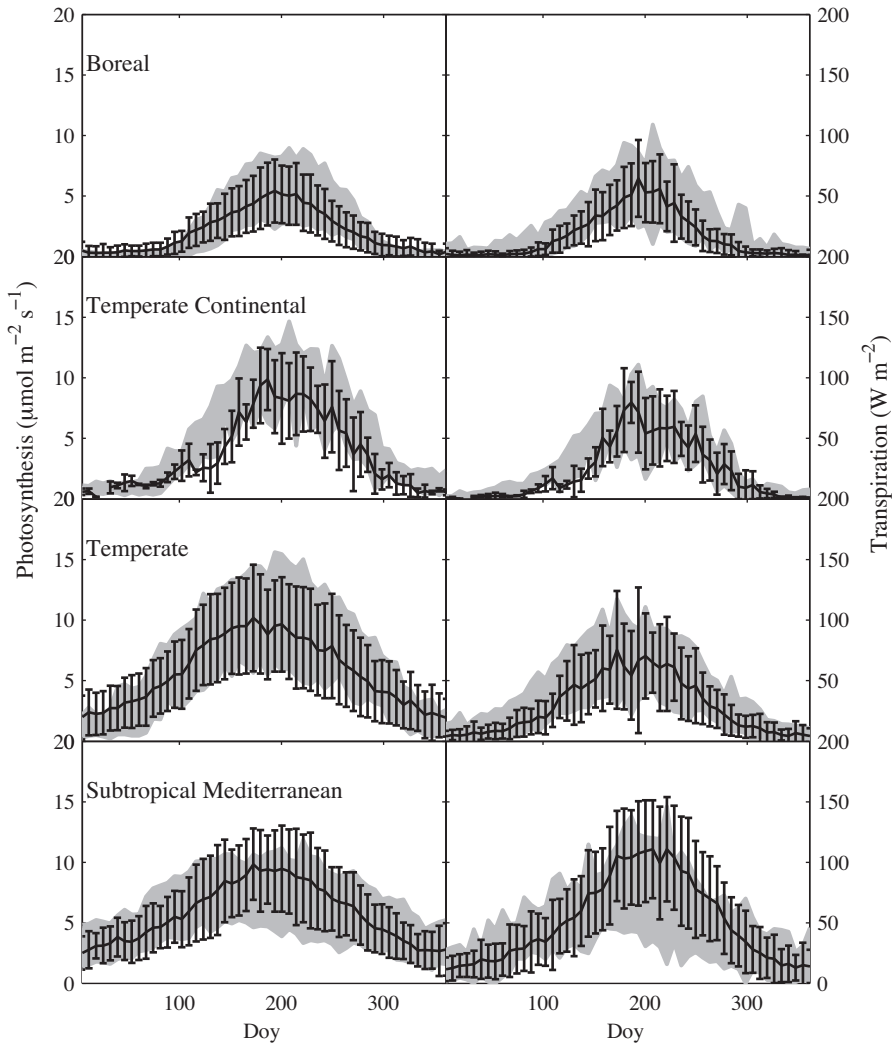

Fig. 4. Seasonal variation of the average weekly observed and simulated photosynthesis (left) and transpiration (right) for the evergreen needle leaf forest sites in four different climates. The fluxes are simulated with parameters derived for each site year (SY). The average observed fluxes with standard deviations are presented by the grey area and the average simulated fluxes with standard deviations by the black lines.

parameters (S) with all sites as in Table 2 and the mean site year parameter (SY) with all years as in Table 3. The different number of parameters within each group will influence the standard deviations and thus their means and standard deviations cannot directly be compared.

The standard deviation (σ) of the parameter values from all site years is an indicator for the variation within a group. With σ the 95% interval confidence intervals in Tables 3 and 4 are estimated. First the standard error is calculated ($\sigma_M = \sigma/\overline{p_1}\sqrt{n}$), which is used to determine the 95% intervals ($p_2 \pm 1.96\sigma_M p_2$), assuming that the parameters are normally distributed. $\overline{p_1}$ is the mean of the site year parameters within a group and p_2 the parameter derived for the group. Cropland parameters have high values for $v_{cm,25}$ and α and a low λ (more efficient water use) (Table 3). This implies that crops are more efficiently assimilating carbon in comparison to other (natural) vegetation types. In contrast, the parameters for savanna, which includes a mixture of grassland, trees and shrubs, imply a low photosynthetic productivity with a high λ. The different forest types show very similar parameter values. The main difference between deciduous and evergreen broadleaf forests is seen for λ, which implies a more efficient water use for the deciduous forests. The two types of evergreen forests show comparable high values for λ. Grassland has an even larger value for λ, while also $v_{cm,25}$ and $j_{m,25}$ are higher than for the different forests.

The quality of the flux simulations are improved only slightly by adding extra model parameters through differentiating vegeta-

Table 3
Model parameters with 95% confidence intervals derived for groups of site years (n) within seven vegetation classes. $v_{cm,25}$ and $j_{m,25}$ in μmol m^{-2} s^{-1}, α and λ in mol mol^{-1}.

	n	$v_{cm,25}$	$j_{m,25}$	α	λ
Cropland	12	48.6 ± 29.9	136.9 ± 33.2	0.27 ± 0.09	150.60 ± 124.8
Savanna	22	18.0 ± 9.7	68.4 ± 35.5	0.11 ± 0.02	593.34 ± 273.0
Deciduous broadleaf forest	63	30.9 ± 8.1	154.9 ± 29.9	0.16 ± 0.02	128.56 ± 33.2
Evergreen broadleaf forest	22	34.3 ± 4.6	114.1 ± 31.3	0.22 ± 0.05	190.77 ± 41.8
Evergreen needleleaf forest	150	27.7 ± 5.2	121.6 ± 13.6	0.16 ± 0.02	209.63 ± 36.1
Grassland	55	43.3 ± 5.0	238.9 ± 31.0	0.10 ± 0.02	276.46 ± 75.4
Mixed forest	25	36.4 ± 11.0	136.2 ± 51.8	0.25 ± 0.05	149.80 ± 131.0

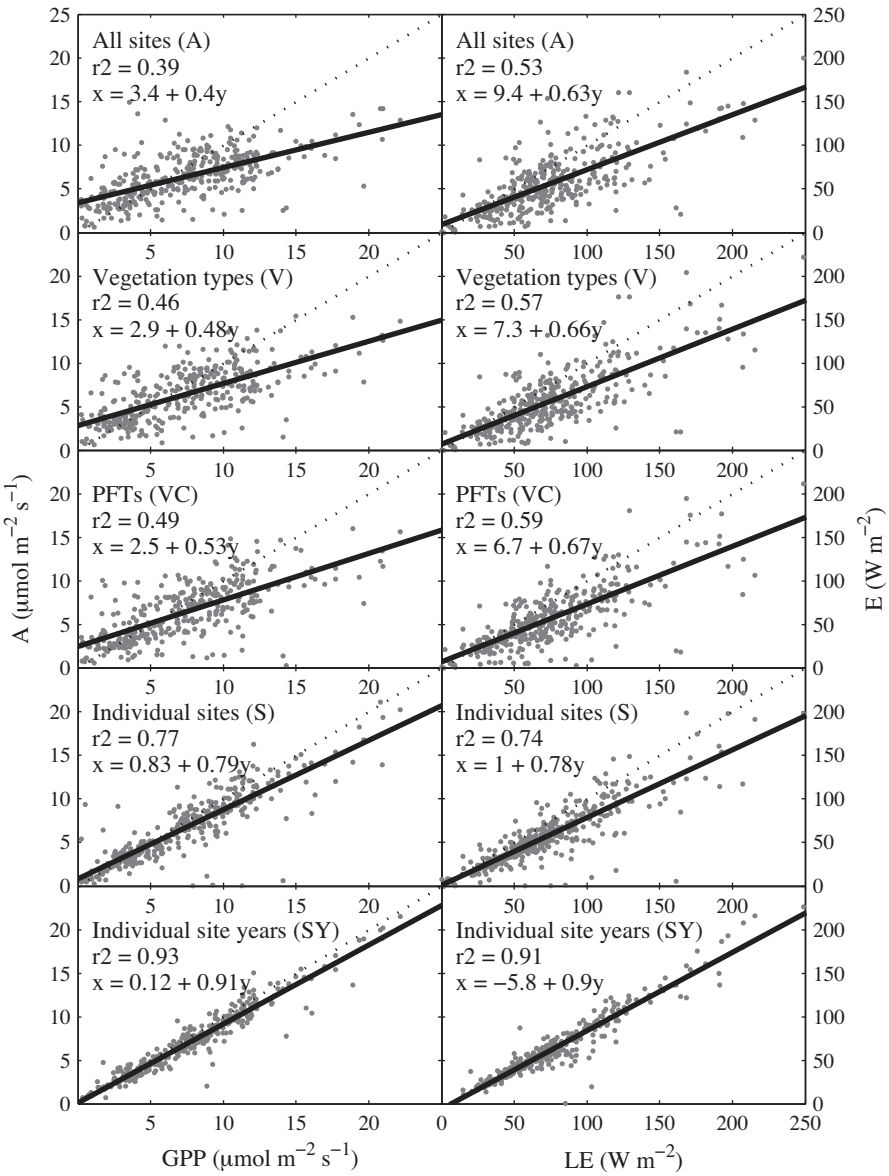

Fig. 5. Comparison of observed and simulated average annual photosynthesis and transpiration fluxes for all site years. Observed fluxes are *GPP* and *LE* and simulated fluxes are *A* and *E*. The dotted line is the 1:1 line and the solid line the regression line. Differences between the panels are the used parameters to simulate the fluxes derived for all sites together (top panels), for groups of sites with a similar vegetation type, for PFTs, for individual sites or for individual site years (lower panels).

tion classes according to climate (compare *V* to VC in Fig. 5). This could suggest that variation of model parameters is not related to climate. In Table 4 the parameters for groups of sites with similar vegetation type and climate (PFTs) are presented to verify this. From this table it is not instantly clear whether a systematic difference exists between climate sub-groups within a PFT. For instance, $v_{cm,25}$ is similar for the climates of evergreen needleleaf forest sites, but variable for the climates of deciduous broadleaf forest sites.

3.3. Grouping sites based on model parameters

Variation of model parameters between PFTs is not coherent (Table 4). The use of this classification results in incorrect simulated fluxes (Fig. 5). Therefore we will attempt to define an independent classification purely based on the model parameters. Hierarchical clustering and *k*-means clustering are both used to group site years with comparable model parameter sets. The choice of the number of groups is subjective, but we chose seven, the same as the number of vegetation types. Different numbers of groups were also tested and these produced comparable results. From Table 5 it can be seen that one large group with 175 site years, and six smaller groups were distinguished when using hierarchical clustering. For *k*-means clustering the groups are more evenly distributed (Table 6). Because the two clustering methods are very sensitive to outliers only those site years are used that are within the range as presented in Fig. 7. Although the groups derived with the two clustering methods are not the same, the patterns as in Fig. 7 are almost identical (data not shown), and thus only the results of *k*-means clustering are discussed further. In Fig. 7 the distribution of the different sites and groups within the parameter space is shown. As expected the groups are clustered around central means. From this figure also the relations between parameters can be seen. For instance, the ratio between $v_{cm,25}$ and $j_{m,25}$ is assumed to be constant in many models. Here both parameters are derived and this results in a ratio of 3.60 ± 1.51 at 25 °C, which is higher than for instance the ratio of 2.0 ± 0.60 as derived by Leuning (2002) from 43 data sets. The parameters $j_{m,25}$ and α are closely linked in Eq. 8, which could result in equifinal simulated fluxes with multiple parameter

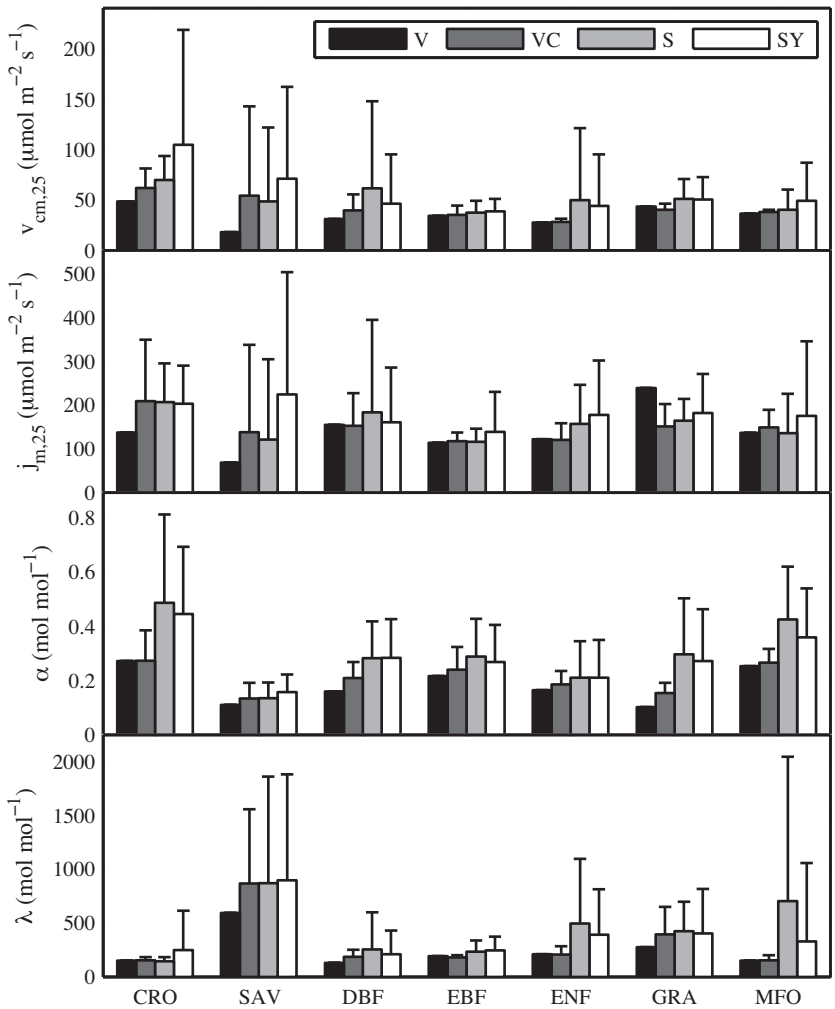

Fig. 6. Mean model parameters and standard deviations for seven vegetation types (as in Table 3) derived for groups of sites with a similar vegetation type (*V*), for PFTs (VC), for individual sites (*S*) or for individual site years (SY).

sets. For group 4 this might be occurring, with low values for α and high values for $j_{m,25}$.

Vegetation type and climate region are not driving factors behind the classification. Each group, derived by *k*-means clustering, contains almost all vegetation types and climate regions (Fig. 8). It is difficult to see clear dominant vegetation types or climate regions within the different groups. Evergreen broadleaf forests are only found in the first three groups, which contain all different climate regions. Groups 4 and 5 both consist of evergreen needleleaf forests and grasslands in boreal and temperate regions. The differences between these groups are a high $j_{m,25}$ and a low λ for group 4, and a low $j_{m,25}$ and a high λ for group 5.

4. Discussion

In global land-surface models parameters are distributed by PFTs (Bonan et al., 2003; Sitch et al., 2003; Krinner et al., 2005). For instance, bioclimatic limits are chosen defining the possibilities for establishment and survival of a given PFT at a certain location, or a temperature response of photosynthesis. We suggest with our findings that model parameters are more variable than are assumed within given PFTs. This finding is supported by statistical grouping of the sites based on the model parameter values. The derived groups could not be related to vegetation type or climate region (Fig. 8). Site years with comparable model parameters do not have a common vegetation type or climate.

This raises the question of what the common characteristics are for these statistically determined groups of sites. These characteristics are essential to provide parameter values for every grid cell in a global land-surface model. One possible hypothesis poses that the parameters are a representation of short term strategies to avoid stress and responses to disturbances to for example drought, heat or a lack of nutrients (Bonan et al., 2003). With this concept differences between the statistical groups may be better understood. The variation will not be detectable when comparing average environmental variables, because in almost all cases stress occurs only during specific short periods. A second possible hypothesis poses that sites cannot be grouped based on the model parameters. PFTs might be changing too abruptly, while in reality the drivers cause a more gradual change. A classification of vegetation can be following these more gradual transitions, comparable to the leaf economics spectrum (Reich et al., 1997; Wright et al., 2004; Harrison et al., 2010). Alternatively, our simple model formulations may not able to capture the variation of processes involved in the global ecosystem carbon and water balance. This could potentially also result in a too large parameter variation within a PFT, that would be an artifact of the modeling approach rather than a real phenomenon. While we think this explanation is rather improbable, we cannot completely discard it either with the current analysis.

The finding that model parameters are more variable than are assumed with the PFTs is supported by the quality of the simulated fluxes, which increases with more specifically defined model

Table 4
Model parameters derived for groups of site years (n) of the PFTs from Table 2. $v_{cm,25}$ and $j_{m,25}$ in μmol m^{-2} s^{-1}, α and λ in mol mol^{-1}. * invalid value of α resulted in incorrect parameters. ** unable to derive confidence intervals due to small sample size.

		n	$v_{cm,25}$	$j_{m,25}$	α	λ
Cropland	Subtr. Med.	5	48.0 ± 15.7	109.3 ± 44.9	0.35 ± 0.08	174.7 ± 101.5
	Temperate	7	75.5 ± 13.9	307.8 ± 97.2	0.19 ± 0.12	131.3 ± 22.7
Savanna	Boreal	4	12.1 ± 2.4	47.0 ± 13.5	0.13 ± 0.01	376.7 ± 94.4
	Subtr. Med.	8	23.3 ± 6.6	81.1 ± 78.0	0.16 ± 0.04	247.4 ± 63.8
	Temperate	1	12.2**	33.6**	0.20**	530.3**
	Temp. Cont.	5	212.6*	493.6*	2.61*	1339.3*
	Tropical	4	10.1 ± 5.5	34.9 ± 24.5	0.06 ± 0.02	1839.5 ± 1794.3
Deciduous broadleaf forest	Boreal	7	28.9 ± 2.4	93.7 ± 21.1	0.18 ± 0.06	279.7 ± 251.3
	Subtr. Med.	21	26.4 ± 4.1	112.6 ± 20.5	0.15 ± 0.03	138.9 ± 34.8
	Temperate	24	40.8 ± 4.8	142.6 ± 28.7	0.23 ± 0.05	146.5 ± 171.4
	Temp. Cont.	11	61.7 ± 8.6	260.4 ± 37.5	0.28 ± 0.05	181.5 ± 42.8
Evergreen broadleaf forest	Subtr. Med.	8	24.6 ± 4.5	95.7 ± 63.0	0.16 ± 0.06	197.2 ± 67.9
	Temperate	3	42.3 ± 4.6	136.5 ± 4.6	0.33 ± 0.13	159.0 ± 107.3
	Tropical	11	38.3 ± 5.9	118.9 ± 28.7	0.23 ± 0.05	186.8 ± 35.2
Evergreen needleleaf forest	Boreal	66	23.7 ± 3.1	113.7 ± 19.8	0.14 ± 0.03	268.9 ± 48.6
	Subtr. Med.	33	27.4 ± 3.3	102.5 ± 23.7	0.18 ± 0.03	277.0 ± 121.7
	Temperate	44	30.6 ± 4.0	175.5 ± 27.3	0.16 ± 0.03	121.1 ± 104.4
	Temp. Cont.	7	30.3 ± 4.0	89.8 ± 13.9	0.26 ± 0.09	162.5 ± 194.4
Grassland	Arctic	2	42.3**	129.1**	0.16**	682.4**
	Subtr. Med.	11	33.3 ± 9.5	113.3 ± 22.9	0.19 ± 0.05	192.6 ± 40.0
	Temperate	42	45.0 ± 4.4	209.7 ± 31.3	0.11 ± 0.02	307.6 ± 60.4
Mixed forest	Subtr. Med.	8	37.6 ± 5.9	178.3 ± 126.7	0.22 ± 0.10	153.5 ± 45.2
	Temperate	8	40.5 ± 5.1	165.8 ± 20.8	0.26 ± 0.08	109.3 ± 47.2
	Temp. Cont.	9	35.7 ± 10.5	103.3 ± 32.0	0.32 ± 0.08	200.1 ± 20.7

Table 5
Average parameters with 95% confidence intervals for the site years (n) within seven groups derived with hierarchical clustering. $v_{cm,25}$ and $j_{m,25}$ in μmol m^{-2} s^{-1}, α and λ in mol mol^{-1}.

	n	$v_{cm,25}$	$j_{m,25}$	α	λ
1	175	40.9 ± 1.8	159.4 ± 9.9	0.26 ± 0.02	176.4 ± 10.2
2	48	31.3 ± 4.2	114.1 ± 16.7	0.16 ± 0.02	413.2 ± 24.2
3	15	32.4 ± 6.2	132.1 ± 23.8	0.12 ± 0.02	697.1 ± 67.3
4	11	53.7 ± 15.6	461.1 ± 36.5	0.18 ± 0.06	163.8 ± 37.8
5	11	94.8 ± 10.0	245.9 ± 31.4	0.60 ± 0.09	214.9 ± 49.1
6	7	58.4 ± 14.6	116.1 ± 23.3	0.75 ± 0.09	213.5 ± 87.3
7	6	58.2 ± 12.6	152.6 ± 41.7	0.62 ± 0.14	655.5 ± 73.8

parameters (Fig. 5). The acceptance of the quality of flux simulations using PFT model parameters in global models depends on the purpose of the simulations. It will be quite different if we want to model a given site to a high degree of precision and accuracy or whether we want a global model to work with prescribed accuracy with a minimum number of parameters.

The quality of the flux simulations and the values of the model parameters are influenced by the quality of the data used and by the model structure. Flux measurements contain random and systematic errors. Random errors result from the equipment used and data processing procedures, such as inaccurate calibrations, high- and low-frequency flux losses. Systematic errors occur because of storage-related problems during low turbulence conditions and advection (Raupach et al., 2005; Richardson et al., 2006, 2008; Lasslop et al., 2008). The model parameters in this study are optimized with eddy covariance flux data and given meteorological data. Parameter uncertainty derived from these observations has been determined by Richardson et al. (2007) – around 5–15% for the parameters of their model – and are comparable between years. The mean absolute weighted error was used to estimate maximum likelihood parameters in their study, because the flux error is approximated by a double-exponential distribution (Richardson and Hollinger, 2005). But according to Lasslop et al. (2008) the flux error distribution follows a superposition of Gaussian distributions. They tested different objective functions, and concluded that there were no significant differences between the least squares optimization with the use of absolute deviations. We use gross primary production (*GPP*) fluxes from the Fluxnet database, which are derived from observed *NEE* by a simple model (Reichstein et al., 2005). This could introduce an additional uncertainty into our results, because we use this flux to derive photosynthesis parameters.

A critical part of the model structure is the upscaling from leaf to ecosystem model parameters based on *LAI*. We use satellite derived values of *LAI*, which is for most sites a representation of a larger area than covered by the eddy covariance flux footprint. Especially when the vegetation representation of the two observations are not in agreement errors will be introduced. In the subtropical Mediterranean region the fluxes are overestimated, particularly during summer. This is a result of the use of annual model parameters which are scaled with *LAI*, which may not be able to describe structural adaptation of vegetation to drought. The poor quality of the simulated fluxes for the savanna sites may be attributed to the fact that this vegetation type consists of a combination of grasslands and trees, with different vegetation characteristics that cannot be scaled up with one single value for *LAI*. This problem has an impact on the variation of model parameters. Further work is needed to quantify this impact, and to investigate other possibilities for the upscaling from leaf to ecosystem.

Table 6
Average parameters with 95% confidence intervals for the site years (n) within seven groups derived with k-means clustering. $v_{cm,25}$ and $j_{m,25}$ in μmol m^{-2} s^{-1}, α and λ in mol mol^{-1}.

	n	$v_{cm,25}$	$j_{m,25}$	α	λ
1	87	35.5 ± 1.6	144.8 ± 9.6	0.20 ± 0.01	163.9 ± 11.3
2	59	50.8 ± 3.0	161.5 ± 14.0	0.38 ± 0.02	167.0 ± 18.8
3	55	29.2 ± 2.7	103.8 ± 11.2	0.17 ± 0.02	363.7 ± 17.8
4	27	50.5 ± 7.7	368.0 ± 34.7	0.16 ± 0.03	182.7 ± 28.0
5	21	34.0 ± 7.5	132.1 ± 26.3	0.12 ± 0.02	663.6 ± 54.8
6	18	79.5 ± 11.8	188.6 ± 36.5	0.67 ± 0.07	213.0 ± 44.3
7	6	58.2 ± 12.6	152.6 ± 41.7	0.62 ± 0.14	655.5 ± 73.8

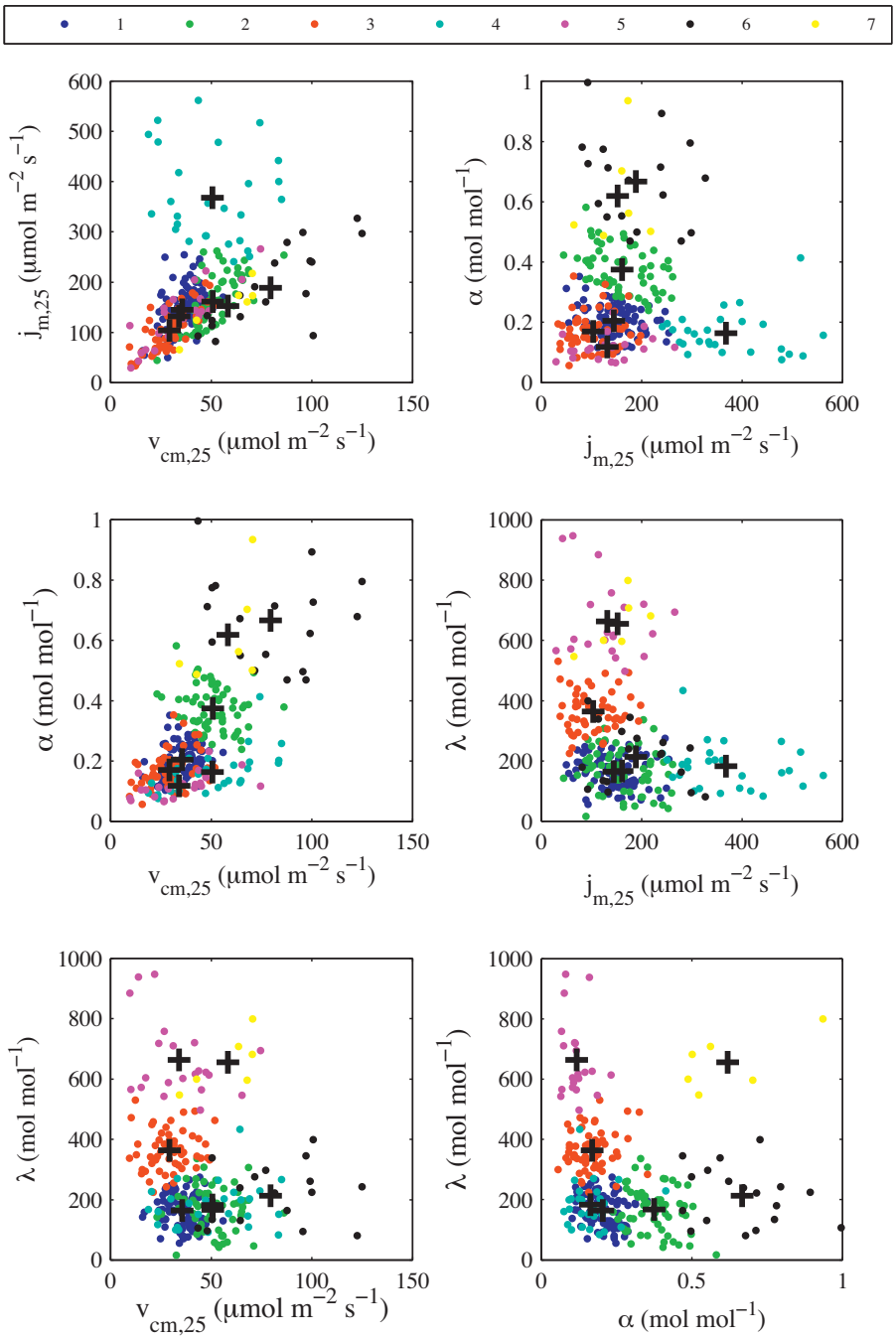

Fig. 7. Model parameters classified by *k*-means clustering. Each point represents a site year, the colors represent different groups and the black crosses represent averages for each group.

The results of our study can only be compared with other studies when taking into account the differences between the model formulations. The values of $v_{cm,25}$ derived by Medlyn et al. (2002b) from measurements on needles from a forest in France are within the same range as the values we derived for needleleaf forests. $v_{cm,25}$ can be compared, because a similar temperature response is used (Eq. 23), although we keep E_{vcm} constant. We assumed a constant temperature response, but Medlyn et al. (2002b) observed a seasonal variation. They compared values of $v_{cm,25}$ and $j_{m,25}$ and found that values were highest for crops and comparable for deciduous and evergreen trees. We derived this variation from the eddy covariance observations. The values derived from the fluxes by Thum et al. (2008) for three forests in Finland and Sweden and by Verbeeck et al. (2008) for a temperate deciduous forest are similar to our results. It is interesting to note here that with both a bottom-up and top-down approach comparable parameter values are derived.

The water use efficiency (λ) is not as frequently used as the parameters from the model of Farquhar et al. (1980). From the definition of λ, given in Eq. 1, it can be seen that a higher λ indicates a lower water use efficiency. Arneth et al. (2006) use the terms conservative and aggressive water use for low and higher values of λ for sites in Siberia and southern Africa. This is what our results show as well, with highest values of λ for the savanna sites. These results are interesting, as the lowest values of λ would be expected at the site with largest water stress. This is consistent with the results of

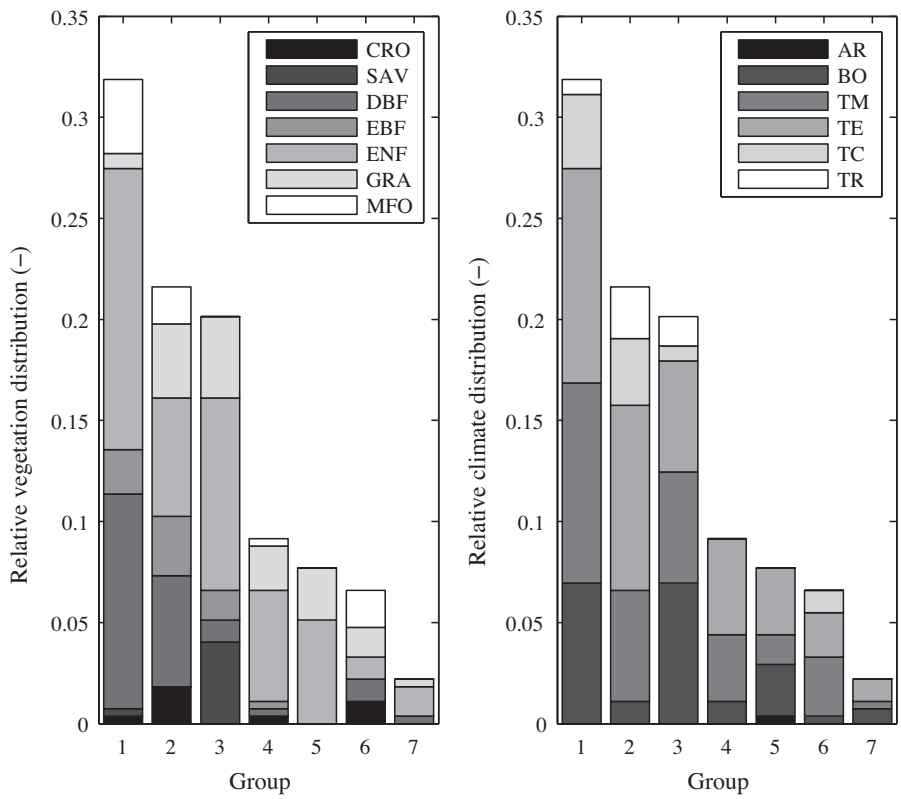

Fig. 8. Distribution of vegetation types and climate regions within groups in Table 6 derived from *k*-means clustering for Model I. Vegetation types are cropland (CRO), savanna (SAV), deciduous broadleaf forest (DBF), evergreen broadleaf forest (EBF), evergreen needleleaf forest (ENF), grassland (GRA) and mixed forest (MFO). Climats are arctic (AR), boreal (BO), subtropical Mediterranean (TM), temperate (TE), temperate continental (TC) and tropical (TR).

Schymanski et al. (2009), who derived a low value for λ during the dry season and higher values during the wet season for a savanna site in Australia.

5. Summary and conclusions

With a simple photosynthesis model we derived parameters for all sites available within the Fluxnet database. The model is capable of simulating the diurnal and seasonal variation of photosynthesis and transpiration fluxes for a large range of sites with different vegetation types and climates. For this no additional site information is needed besides the eddy covariance fluxes, meteorological data and seasonal *LAI*, the simplified approach allowing us to apply the model at all sites.

The choice of a parameter classification has a large impact on the quality of the simulated photosynthesis and transpiration fluxes. When more general parameters are used, the quality of the fluxes decreases. The diurnal and seasonal cycles and annual average fluxes are over- or underestimated. The best fluxes are simulated with parameters that are derived for each individual site year. This indicates that a PFT classification introduces an uncertainty to the short term variation of photosynthesis and transpiration fluxes.

We conclude that model parameters are more variable than assumed with the PFTs. A PFT classification does not reflect reality of short term photosynthesis and transpiration flux variation, supporting that a more dynamic description of trait-based PFTs is a necessary next step. Site years with comparable model parameters do not have a common vegetation type or climate. The derived groups could not be related to vegetation type or climate region. Although site year parameters produce the best results, this generates a different problem. The parameters are too specific to be used in a global study, but they can be used to explore the possibilities of an alternative classification scheme. The question as to whether it is possible to classify sites, or if a more fine scaled methodology with gradual transitions is needed is still open. Further work is needed before a classification of vegetation within a global climate model can be produced.

Acknowledgements

This work is the outcome of the La Thuile Fluxnet workshop 2007, which received financial support of CarboEuropeIP, FAO-GTOS-TCO, iLEAPS, Max Planck Institute for Biogeochemistry, National Science Foundation, University of Tuscia, US Department of Energy. We acknowledge database and technical support from Berkeley Water Center, Lawrence Berkeley National Laboratory, Microsoft Research eScience, Oak Ridge National Laboratory, University of California-Berkeley, University of Virginia. The authors gratefully acknowledge the collection of the Fluxnet database by all people involved. Without this global data this research would not have been possible. The following networks participated with flux data: AmeriFlux, AfriFlux, AsiaFlux, CarboAfrica, CarboEuropeIP, ChinaFlux, Fluxnet-Canada, KoFlux, LBA, NECC, OzFlux, TCOS-Siberia, USCCC. B.E. Law is acknowledged for her work on the AmeriFlux database as part of the AmeriFlux Science Team Research grant (US Department of Energy, Terrestrial Carbon program Award DE-FG02-04ER63911). The Metolius AmeriFlux research and research at the MMSF site was supported by the Office of Science (BER), U.S. Department of Energy, Grant No. DE-FG02-06ER64318 and DE-FG02-07ER64371. This research is funded by a grant from the Netherlands Organization for Scientific Research (NWO).

Appendix A. Model description

A.1. Photosynthesis and transpiration

Photosynthesis is simulated with a biochemical model based on the work of Farquhar et al. (1980). Leaf photosynthesis (A) is the minimum of carboxylation (W_c) and Ribulose-1,5-bisphosphate (RuBP) regeneration (W_j) minus respiration (R_d).

$$A = \left(1 - \frac{\Gamma^*}{C_i}\right) \min\{W_c, W_j\} - R_d \tag{3}$$

where Γ^* is the compensation point for CO_2 in absence of dark respiration (bar) and C_i the intercellular partial pressure of CO_2 (bar) and $R_d = 0.07V_{cm}$. W_c and W_j are determined with the following equations (Farquhar et al., 1980; von Caemmerer and Farquhar, 1981):

$$W_c = \frac{V_{cm}C_i}{C_i + k'} \tag{4}$$

$$W_j = \frac{JC_i}{4(C_i + 2\Gamma^*)} \tag{5}$$

$$k' = K_c(1 + O/K_o) \tag{6}$$

$$\Gamma^* = 0.5\frac{V_{om}}{V_{cm}}\frac{K_c}{K_o O} \tag{7}$$

$$J = \frac{\alpha I_{PAR} J_m}{\alpha I_{PAR} + 2.1J_m} \tag{8}$$

where I_{PAR} is the photosynthetic active radiation (μmol photons m^{-2} s^{-1}), J the electron yield, V_{cm} the rate of carboxylation mediated by the enzyme Rubisco (μmol m^{-2} s^{-1}), V_{om} the rate of oxygenation of Rubisco (μmol m^{-2} s^{-1}), J_m the maximum potential electron transport rate (μmol m^{-2} s^{-1}), α the quantum yield (mol mol^{-1}), K_c the kinetic coefficient for CO_2 (bar), K_o the kinetic coefficient for O_2 (bar) and O the partial pressure for O_2 (bar). The ratio V_{om}/V_{cm} is assumed to be a constant of 0.21.

The reduction of photosynthesis when soil water is limited, is simulated by multiplying the right hand side of Eq. 3 by a factor β, which ranges between 0 and 1 (Matsumoto et al., 2008):

$$\beta = \frac{(\theta - \theta_{\min})(\theta_{\max} - \theta_{\min} + \beta_1)}{(\theta_{\max} - \theta_{\min})(\theta - \theta_{\min} + \beta_1)} \tag{9}$$

$$A = \beta[(1 - \Gamma^*/c_i)\min\{W_c, W_j\} - R_d] \tag{10}$$

where θ is the soil water content (%), $\theta_{\min}$ and $\theta_{\max}$ are the minimum and maximum volumetric soil water content observed at a site and β_1 is a parameter used to fit an envelope curve around the soil water content observations. With β both photosynthesis and transpiration are reduced during dry periods.

Transpiration (E) is a function of stomatal conductance (g_s), which can be calculated from A, c_a and c_i (ppm):

$$g_s = \frac{A}{c_a - c_i} \tag{11}$$

$$E = 1.6Dg_s \tag{12}$$

where D is the molar vapor gradient between stomata and the air and 1.6 the ratio of molecular diffusivity of H_2O to CO_2.

The internal partial pressure of CO_2 (c_i) is determined as described by Arneth et al. (2002), where the models of Cowan (1977) and Farquhar et al. (1980) are combined, by solving the following quadratic equation:

$$k_2C_i^2 + k_1C_i + k_0 = 0 \tag{13}$$

There are two sets of solutions for the k parameters, under enzyme-limited conditions (W_c) and light-limited conditions (W_j). In the enzyme-limited case the values for the k parameters are calculated with the following equations:

$$k_2 = \lambda - \frac{1.6D}{k' + \Gamma^*} \tag{14}$$

$$k_1 = 1.6D - 2\lambda C_a + \frac{1.6D(\Gamma^* - k')}{k' + \Gamma^*} \tag{15}$$

$$k_0 = (\lambda C_a - 1.6D)C_a + \frac{1.6D\Gamma^* k'}{k' + \Gamma^*} \tag{16}$$

and in the light-limited case by:

$$k_2 = \lambda - \frac{1.6D}{3\Gamma^*} \tag{17}$$

$$k_1 = 1.6D - 2\lambda C_a - \frac{1.6D\Gamma^*}{3\Gamma^*} \tag{18}$$

$$k_0 = (\lambda C_a - 1.6D)C_a + \frac{1.6D2\Gamma^{*2}}{3\Gamma^*} \tag{19}$$

where C_a is the partial pressure of ambient CO_2 (bar) and λ the ratio between E and A as a function of g_s (mol mol^{-1}).

A.2. Scaling up from leaf to canopy

In most models scaling up is based on the assumption that the profile of leaf nitrogen content along the depth of the canopy follows the time-mean profile of radiation (Sellers et al., 1992; Arora, 2002). The main assumption is that the photosynthetic properties of leaves acclimate fully to the light conditions within a canopy. The photosynthetic capacity is proportional to the time-integrated absorbed radiation (Kull and Jarvis, 1995). Photosynthetically active radiation (*PAR*) is assumed to be the only variable determining change in the values of parameters within the canopy. The exponential light interception model holds:

$$I(x) = I_0 \times e^{-kL(x)} \tag{20}$$

where I_0 is the *PAR* incident on top of the canopy, $L(x)$ is the leaf area index cumulated from the top of the canopy down to level x, $I(x)$ is the *PAR* at level x within the canopy and k is a function of the leaf inclination angle distribution. Total *PAR* absorbed by the canopy (I_C) can be obtained by integrating Eq. 20 over the depth of the canopy, which results in:

$$I_C = I_0 \times \frac{(1 - e^{-kL})}{k} \tag{21}$$

Parameters that determine the photosynthesis rate follow the same exponential function. This implies that these parameters can be scaled up from the leaf to the canopy in a similar way (Cox et al., 1998; Wolf et al., 2006):

$$P = p \times \frac{(1 - e^{-kL})}{k} \tag{22}$$

where P is the canopy scale parameter and p the leaf scale parameter. This function applies for the canopy scale parameters V_{cm}, J_m and α_c which are derived from the temperature corrected parameters at the leaf scale (v_{cm}, j_m and α). k is set to 0.5 for all sites. λ is not scaled with *LAI* as it is parameterized on the ecosystem scale.

A.3. Temperature responses

At the leaf scale there are several studies in which the temperature response of v_{cm} and j_m are determined from observations (Bunce, 2000; Medlyn et al., 2002a,b; Kattge and Knorr, 2007). The parameters are described by an Arrhenius function or modified Arrhenius function with an optimal temperature. These different models have been validated at the leaf scale, but at the ecosystem scale there are no observations as the parameters are the sum of

the individual leaves. The temperature response function that will be used in this study is (Knorr and Kattge, 2005; Thum et al., 2008):

$$p = p_{25} \times \exp\left\{\frac{E_p(T - T_{ref})}{T_{ref}RT}\right\} \tag{23}$$

This function applies for the parameters v_{cm}, j_m, K_C and K_O, for which $v_{cm,25}$, $j_{m,25}$, $K_{C,25}$ and $K_{O,25}$ are the parameter values at the reference temperature (T_{ref} = 25 °C), $E_{v_{cm}}$, E_{j_m}, E_C and E_O the activation energies, T the temperature [K] and R the gas constant.

Appendix B. Characteristics of the Fluxnet sites used in this study

See Table B.1.

Table B.1
The site name codes are a composition of country (first two letters) and site name (last three letters). Vegetation types are closed shrubland (CSH), cropland (CRO), deciduous broadleaf forest (DBF), evergreen broadleaf forest (EBF), evergreen needleleaf forest (ENF), grassland (GRA), mixed forest (MFO), open shrubland (OSH), savanna (SAV), wetland (WET) and woody savanna (WSA). Climates are arctic (AR), boreal (BO), subtropical Mediterranean (SM), temperate (TE), temperate continental (TC) and tropical (TR). References are given describing the sites, when no reference was available the site researcher is named.

Site	Climate	Vegetation	Latitude	Longitude	Reference
AT-Neu	TE	GRA	47.12	11.32	Wohlfahrt et al. (2008)
AU-Fog	TR	SAV	−12.54	131.31	Jason Beringer
AU-Wac	TE	EBF	−37.43	145.19	Wood et al. (2008)
BE-Jal	TE	MF	50.56	6.07	Louis François
BE-Vie	TE	MF	50.31	6.00	Aubinet et al. (2001)
BR-Ban	TR	EBF	−9.82	−50.16	da Rocha et al. (2009)
BR-Sp1	TR	WSA	−21.62	−47.65	Santos et al. (2004)
CA-Ca1	TE	ENF	49.87	−125.33	Humphreys et al. (2006)
CA-Ca2	TE	ENF	49.87	−125.29	Humphreys et al. (2006)
CA-Ca3	TE	ENF	49.53	−124.90	Humphreys et al. (2006)
CA-Mer	TC	OSH	45.41	−75.52	Lafleur et al. (2003)
CA-NS3	BO	ENF	55.91	−98.38	Goulden et al. (2006)
CA-NS4	BO	ENF	55.91	−98.38	Goulden et al. (2006)
CA-NS5	BO	ENF	55.86	−98.49	Goulden et al. (2006)
CA-NS6	BO	OSH	55.92	−98.96	Goulden et al. (2006)
CA-Oas	BO	DBF	53.63	−106.20	Black et al. (2000)
CA-Obs	BO	ENF	53.99	−105.12	Krishnan et al. (2008)
CA-Ojp	BO	ENF	53.92	−104.69	Howard et al. (2004)
CA-Qcu	BO	ENF	49.27	−74.04	Giasson et al. (2006)
CA-Qfo	BO	ENF	49.69	−74.34	Bergeron et al. (2007)
CA-SF1	BO	ENF	54.49	−105.82	Mkhabela et al. (2009)
CA-SF2	BO	ENF	54.25	−105.88	Mkhabela et al. (2009)
CA-SF3	BO	ENF	54.09	−106.01	Mkhabela et al. (2009)
CA-SJ1	BO	ENF	53.91	−104.66	Zha et al. (2009)
CA-SJ2	BO	ENF	53.95	−104.65	Zha et al. (2009)
CA-SJ3	BO	ENF	53.88	−104.65	Zha et al. (2009)
CA-TP4	TC	ENF	42.71	−80.36	Arain and Restrepo-Coupe (2005)
CH-Oe1	TE	GRA	47.29	7.73	Ammann et al. (2007)
CN-Cha	TC	MF	42.4	128.1	Guan et al. (2006)
CN-Do2	SM	GRA	31.58	121.9	Yan et al. (2008)
CN-HaM	AR	GRA	37.37	101.18	Kato et al. (2006)
DE-Hai	TE	DBF	51.08	10.45	Knohl et al. (2003)
DE-Kli	TE	CRO	50.89	13.52	Christian Bernhofer
DE-Tha	TE	ENF	50.96	13.57	Grünwald and Berhofer (2007)
DE-Wet	TE	ENF	50.45	11.46	Rebmann et al. (2010)
DK-Lva	TE	GRA	55.68	12.08	Gilmanov et al. (2007)
DK-Sor	TE	DBF	55.49	11.65	Pilegaard et al. (2003)
ES-ES1	SM	ENF	39.35	−0.32	Sanz et al. (2004)
ES-ES2	SM	CRO	39.28	−0.32	Maria Jose Sanz
ES-LMa	SM	SAV	39.94	−5.77	Maria Jose Sanz
ES-VDA	TE	GRA	42.15	1.45	Gilmanov et al. (2007)
FI-Hyy	BO	ENF	61.85	24.29	Suni et al. (2003b)
FI-Sod	BO	ENF	67.36	26.64	Suni et al. (2003a)
FR-Fon	TE	DBF	48.48	2.78	Eric Dufrêne
FR-LBr	TE	ENF	44.72	−0.77	Berbigier et al. (2001)
FR-Lq1	TE	GRA	45.64	2.74	Gilmanov et al. (2007)
FR-Lq2	TE	GRA	45.64	2.74	Gilmanov et al. (2007)
GF-Guy	TR	EBF	5.28	−52.93	Bonal et al. (2008)
HU-Mat	TE	GRA	47.85	19.73	Pintér et al. (2008)
ID-Pag	TR	EBF	2.35	114.04	Hirano et al. (2007)
IE-Dri	TE	GRA	51.99	−8.75	Gerard Kiely
IT-Amp	SM	GRA	41.9	13.61	Gilmanov et al. (2007)
IT-BCi	SM	CRO	40.52	14.96	Reichstein et al. (2003a)
IT-Col	SM	DBF	41.85	13.59	Valentini et al. (1996)
IT-Cpz	SM	EBF	41.71	12.38	Garbulksy et al. (2008)
IT-Lav	TE	ENF	45.96	11.28	Marcolla et al. (2003)
IT-Lec	SM	EBF	43.3	11.27	Lorenzo Genesio
IT-LMa	TE	DBF	45.58	7.15	Fabio Petrella
IT-Mal	TE	GRA	46.12	11.7	Gilmanov et al. (2007)
IT-MBo	TE	GRA	46.02	11.05	Gianelle et al. (2009)
IT-Non	SM	DBF	44.69	11.09	Reichstein et al. (2003a)
IT-Pia	SM	OSH	42.58	10.08	Reichstein et al. (2005)

Table B.1 (*Continued*)

Site	Climate	Vegetation	Latitude	Longitude	Reference
IT-Ren	TE	ENF	46.59	11.43	Montagnani et al. (2009)
IT-Ro1	SM	DBF	42.41	11.93	Rey et al. (2002)
IT-SRo	SM	ENF	43.73	10.28	Chiesi et al. (2005)
JP-Tom	TC	MF	42.74	141.51	Hirata et al. (2007)
NL-Ca1	TE	GRA	51.97	4.93	Jacobs et al. (2007)
NL-Ca2	TE	CRO	51.95	4.9	Jacobs et al. (2007)
NL-Loo	TE	ENF	52.17	5.74	Dolman et al. (2002)
SE-Faj	TE	WET	56.27	13.55	Lund et al. (2007)
SE-Nor	TC	ENF	60.09	17.48	Lagergren et al. (2008)
SK-Tat	TC	ENF	49.12	20.16	Dario Papale
UK-EBu	TE	GRA	55.87	−3.21	Mark Sutton
UK-ESa	TE	CRO	55.91	−2.86	John Moncrieff
UK-Gri	TE	ENF	56.61	−3.8	Rebmann et al. (2005)
UK-Ham	TE	DBF	51.12	−0.86	Mike Broadmeadow
UK-PL3	TE	DBF	51.45	−1.27	Richard Harding
US-Bar	TC	DBF	44.06	−71.29	Jenkins et al. (2007)
US-Blo	SM	ENF	38.9	−120.63	Misson et al. (2005)
US-Bn1	BO	ENF	63.92	−145.38	Liu et al. (2005)
US-Bn2	BO	DBF	63.92	−145.38	Liu et al. (2005)
US-CaV	TE	GRA	39.06	−79.42	Tilden Meyers
US-Dk2	SM	MF	35.97	−79.1	Pataki and Oren (2003)
US-Dk3	SM	MF	35.98	−79.09	Pataki and Oren (2003)
US-Goo	SM	GRA	34.25	−89.97	Tilden Meyers
US-KS1	SM	ENF	28.46	−80.67	Bert Drake
US-KS2	SM	CSH	28.61	−80.67	Powell et al. (2006)
US-Me1	SM	ENF	44.58	−121.5	Irvine et al. (2007)
US-Me3	SM	ENF	44.32	−121.61	Vickers et al. (2009)
US-Me4	SM	ENF	44.5	−121.62	Anthoni et al. (2002)
US-MMS	SM	DBF	39.32	−86.41	Schmid et al. (2000)
US-MOz	SM	DBF	38.74	−92.2	Gu et al. (2006)
US-NC2	SM	ENF	35.8	−76.67	Noormets et al. (2010)
US-NR1	BO	ENF	40.03	−105.55	Monson et al. (2002)
US-Syv	TC	MF	46.24	−89.35	Desai et al. (2005)
US-WCr	TC	DBF	45.81	−90.08	Cook et al. (2004)
US-Wi1	TC	DBF	46.73	−91.23	Noormets et al. (2007)
US-Wi4	TC	ENF	46.74	−91.17	Noormets et al. (2007)
US-Wi8	TC	DBF	46.72	−91.25	Noormets et al. (2007)
US-Wrc	TC	ENF	45.82	−121.95	Falk et al. (2008)
VU-Coc	TR	EBF	−15.44	167.19	Roupsard et al. (2006)

References

Ammann, C., Flechard, C., Leifeld, J., Neftel, A., Fuhrer, J., 2007. The carbon budget of newly established temperate grassland depends on management intensity. Agric. Ecosyst. Environ. 121, 5–20.

Anthoni, P.M., Unsworth, M.H., Law, B.E., Irvine, J., Baldocchi, D.D., Van Tuyl, S., Moore, D., 2002. Seasonal differences in carbon and water vapor exchange in young and old-growth ponderosa pine ecosystems. Agric. Forest Meteorol. 111, 203–222.

Arain, M.A., Restrepo-Coupe, N., 2005. Net ecosystem production in a temperate pine plantation in southeastern Canada. Agric. Forest Meteorol. 128, 223–241.

Arneth, A., Lloyd, J., Šantrůčková, H., Bird, M., Grigoryev, S., Kalaschnikov, Y.N., Gleixner, G., Schulze, E.D., 2002. Response of central Siberian Scots pine to soil water deficit and long-term trends in atmospheric CO_2 concentration. Global Biogeochem. Cycles 16, 1005.

Arneth, A., Sitch, S., Bondeau, A., Butterbach-Bahl, K., Foster, P., Gedney, N., de Noblet-Ducoudré, N., Prentice, I.C., Sanderson, M., Thonicke, K., Wania, R., Zaehle, S., 2010. From biota to chemistry and climate: towards a comprehensive description of trace gas exchange between the biosphere and atmosphere. Biogeosciences 7, 121–149.

Arneth, A., Veenendaal, E.M., Best, C., Timmermans, W., Kolle, O., Montagnani, L., Shibistova, O., 2006. Water use strategies and ecosystem–atmosphere exchange of CO_2 in two highly seasonal environments. Biogeosciences 3, 421–437.

Arora, V., 2002. Modeling vegetation as a dynamic component in soil–vegetation–atmosphere transfer schemes and hydrological models. Rev. Geophys. 40, 3.

Aubinet, M., Chermanne, B., Vandenhaute, M., Longdoz, B., Yernaux, M., Laitat, E., 2001. Long term carbon dioxide exchange above a mixed forest in the Belgian Ardennes. Agric. Forest Meteorol. 108, 293–315.

Aubinet, M., Grelle, A., Ibrom, A., Rannik, Ü., Moncrieff, J., Foken, T., Kowalski, A.S., Martin, P.H., Berbigier, P., Bernhofer, C., Clement, R., Elbers, J., Granier, A., Grünwald, T., Morgenstern, K., Pilegaard, K., Rebmann, C., Snijders, W., Valentini, R., Vesala, T., 2000. Estimates of the annual net carbon and water exchange of forests: the EUROFLUX methodology. Adv. Ecol. Res. 30, 113–175.

Baldocchi, D., 2008. TURNER REVIEW No. 15. 'Breathing' of the terrestrial biosphere: lessons learned from a global network of carbon dioxide flux measurement systems. Aust. J. Bot. 56, 1–26.

Baldocchi, D., Falge, E., Gu, L., Olson, R., Hollinger, D., Running, S., Anthoni, P., Bernhofer, Ch., Davis, K., Evans, R., Fuentes, J., Goldstein, A., Katul, G., Law, B., Lee, X., Mahli, Y., Meyers, T., Munger, W., Oechel, W., Paw U, K.T., Pilegaard, K., Schmid, H.P., Valentini, R., Verma, S., Vesala, T., Wilson, K., Wofsy, S., 2001. FLUXNET: a new tool to study the temporal and spatial variability of ecosystem-scale carbon dioxide, water vapor, and energy flux densities. Bull. Am. Meteorol. Soc. 82, 2415–2434.

Beer, C., Ciais, P., Reichstein, M., Baldocchi, D., Law, B.E., Papale, D., Soussana, J.F., Ammann, C., Buchmann, N., Frank, D., Gianelle, D., Janssens, I.A., Knohl, A., Köstner, B., Moors, E., Roupsard, O., Verbeeck, H., Vesala, T., Williams, C.A., Wohlfahrt, G., 2009. Temporal and among-site variability of inherent water use efficiency at the ecosystem level. Global Biogeochem. Cycles 23, GB2018.

Berbigier, P., Bonnefond, J.M., Mellmann, P., 2001. CO_2 and water vapour fluxes for 2 years above Euroflux forest site. Agric. Forest Meteorol. 108, 183–197.

Bergeron, O., Margolis, H.A., Black, T.A., Coursolle, C., Dunn, A.L., Barr, A.G., Wofsy, S.C., 2007. Comparison of carbon dioxide fluxes over three boreal black spruce forests in Canada. Global Change Biol. 13, 89–107.

Black, T.A., Chen, W.J., Barr, A.G., 2000. Increased carbon sequestration by a boreal deciduous forest in years with a warm spring. Geophys. Res. Lett. 27, 1271–1274.

Bonal, D., Bosc, A., Ponton, S., Goret, J.Y., Burban, B., Gross, P., Bonnefond, J.M., Elbers, J., Longdoz, B., Epron, D., Guehl, J.M., Granier, A., 2008. Impact of severe dry season on net ecosystem exchange in the Neotropical rainforest of French Guiana. Global Change Biol. 14, 1917–1933.

Bonan, G.B., Levin, S., Kergoat, L., Oleson, K.W., 2002. Landscapes as patches of plant functional types: An integrating concept for climate and ecosytem models. Global Biogeochem. Cycles 16, 5.

Bonan, G.B., Levis, S., Sitch, S., Vertenstein, M., Oleson, K.W., 2003. A dynamic global vegetation model for use with climate models: concepts and description of simulated vegetation dynamics. Global Change Biol. 9, 1543–1566.

Box, E.O., 1996. Plant functional types and climate at the global scale. J. Veg. Sci. 7, 309–320.

Bunce, J.A., 2000. Acclimation of photosynthesis to temperature in eight cool and warm climate herbaceous C_3 species: Temperature dependence of parameters of a biochemical photosynthesis model. Photosynth. Res. 63, 59–67.

Chapin, F.S., Bret-Harte, M.S., Hobbie, S.E., Zhong, H., 1996. Plant functional types as predictors of transient responses of arctic vegetation to global change. J. Veg. Sci. 7, 347–358.

Chiesi, M., Maselli, F., Bindi, M., Fibbi, L., Cherubina, P., Arlotta, E., Tirone, G., Matteucci, G., Seufert, G., 2005. Modelling carbon budget of Mediterranean forests using ground and remote sensing measurements. Agric. Forest Meteorol. 135, 22–34.

Cook, B.D., Davis, K.J., Wang, W., Desai, A., Berger, B.W., Teclaw, R.M., Martin, J.G., Bolstad, P.V., Bakwin, P.S., Yi, C., Heilman, W., 2004. Carbon exchange and venting anomalies in an upland deciduous forest in northern Wisconsin, USA. Agric. Forest Meteorol. 126, 271–295.

Cowan, I.R., 1977. Stomatal behaviour and environment. Adv. Bot. Res. 4, 117–228.

Cox, P.M., Betts, R.A., Jones, C.D., Spall, S.A., Totterdell, I.J., 2000. Acceleration of global warming due to carbon-cycle feedbacks in a coupled climate model. Nature 408, 184–187.

Cox, P.M., Huntingford, C., Harding, R.J., 1998. A canopy conductance and photosynthesis model for use in a GCM land surface scheme. J. Hydrol. 212–213, 79–94.

da Rocha, H.R., Manzi, A.O., Cabral, O.M., Miller, S.D., Goulden, M.L., Saleska, S.R., Restrepo-Coupe, N., Wofsy, S.C., Borma, L.S., Artaxo, P., Vourlitis, G., Nogueira, Cardoso, F.L., Nobre, A.D., Kruijt, B., Freitas, H.C., von Randow, C., Aguiar, R.G., Maia, J.F., 2009. Patterns of water and heat flux across a biome gradient from tropical forest to savanna in Brazil. J. Geophys. Res. G: Biogeosci. 114, G00B12.

Desai, A.R., Bolstad, P.V., Cook, B.D., Davis, K.J., Carey, E.V., 2005. Comparing net ecosystem exchange of carbon dioxide between an old-growth and mature forest in the upper Midwest, USA. Agric. Forest Meteorol. 128, 33–55.

Dickinson, R.E., Sellers, A.H., Kennedy, P.J., Wilson, M.F., 1986. Biosphere atmosphere transfer scheme (BATS) for the NCAR community climate model. NCAR technical note TN275+STR. 69 pp.

Dolman, A.J., Moors, E.J., Elbers, J.A., 2002. The carbon uptake of a mid latitude forest on sandy soil. Agric. Forest Meteorol. 111, 157–170.

Falk, M., Wharton, S., Schroeder, M., Ustin, S., Paw U, K.T., 2008. Flux partitioning in an old-growth forest: seasonal and interannual dynamics. Tree Physiol. 28, 509–520.

Farquhar, G.D., von Caemmerer, S., Berry, J.A., 1980. A biochemical model of photosynthetic CO_2 assimilation in leaves of C_3 species. Planta 149, 78–90.

Foley, J.A., Levis, S., Prentice, I.C., Pollard, D., Thompson, S.L., 1998. Coupling dynamic models of climate and vegetation. Global Change Biol. 4, 561–579.

Friend, A.D., Arneth, A., Kiang, N.Y., Lomas, M., Ogée, J., Rödenbeck, C., Running, S.W., Santaren, J.D., Sitch, S., Viovy, N., Woodward, F.I., Zaehle, S., 2007. FLUXNET and modelling the global carbon cycle. Global Change Biol. 13, 610–633.

Friend, A.D., Cox, P.M., 1995. Modelling the effects of atmospheric CO_2 on vegetation–atmosphere interactions. Agric. Forest Meteorol. 73, 285–295.

Garbulksy, M.F., Penuelas, J., Papale, D., Fillela, I., 2008. Remote estimation of carbon dioxide uptake by a Mediterranean forest. Global Change Biol. 14, 2860–2867.

Gianelle, D., Vescovo, L., Marcolla, B., Manca, G., Cescatti, A., 2009. Ecosystem carbon fluxes and canopy spectral reflectance of a mountain meadow. Int. J. Rem. Sens. 30, 435–449.

Giasson, M.A., Coursolle, C., Margolis, H.A., 2006. Ecosystem-level CO_2 fluxes from a boreal cutover in eastern Canada before and after scarification. Agric. Forest Meteorol. 140, 23–40.

Gilmanov, T.G., Soussana, J.F., Aires, L., Allard, V., Ammann, C., Balzarolo, M., Barcza, Z., Bernhofer, C., Campbell, C.L., Cernusca, A., Cescatti, A., Clifton-Brown, J., Dirks, B.O.M., Dore, S., Eugster, W., Fuhrer, J., Gimeno, C., Gruenwald, T., Haszpra, L., Hensen, A., Ibrom, A., Jacobs, A.F.G., Jones, M.B., Lanigan, G., Laurila, T., Lohila, A., Manca, G., Marcolla, B., Nagy, Z., Pilegaard, K., Pinter, K., Pio, C., Raschi, A., Rogiers, N., Sanz, M.J., Stefani, P., Sutton, M., Tuba, Z., Valentini, R., Williams, M.L., Wohlfahrt, G., 2007. Partitioning European grassland net ecosystem CO_2 exchange into gross primary productivity and ecosystem respiration using light response function analysis. Agric. Ecosyst. Environ. 121, 93–120.

Goulden, M.L., Winston, G.C., McMillan, A.M.S., Litvak, M.E., Read, E.L., Rocha, A.V., Elliot, J.R., 2006. An eddy covariance mesonet to measure the effect of forest age on land–atmosphere exchange. Global Change Biol. 12, 2146–2162.

Grünwald, T., Berhofer, C., 2007. A decade of carbon, water and energy flux measurements of an old spruce forest at the Anchor Station Tharandt. Tellus 59B, 387–396.

Gu, L., Meyers, T., Pallardy, S.G., Hanson, P.J., Yang, B., Heuer, M., Hosman, K.P., Riggs, J.S., Sluss, D., Wullschleger, S.D., 2006. Direct and indirect effects of atmospheric conditions and soil moisture on surface energy partitioning revealed by a prolonged drought at a temperate forest site. J. Geophys Res. D: Atmos. 111, 16102.

Guan, D.X., Wu, J.B., Zhao, X.S., Han, S.J., Yu, G.R., Sun, X.M., Jin, C.J., 2006. CO_2 fluxes over an old, temperate mixed forest in northeastern China. Agric. Forest Meteorol. 137, 138–149.

Harrison, S.P., Prentice, I.C., Barboni, D., Kohfeld, K.E., Ni, J., Sutra, J.P., 2010. Ecophysiological and bioclimatic foundations for a global plant functional classification. J. Veg. Sci. 21, 300–317.

Hirano, T.H., Segah, H., Harada, T., Limin, S., June, T., Hirata, R., Osaki, M., 2007. Carbon dioxide balance of a tropical peat swamp forest in Kalimantan, Indonesia. Global Change Biol. 13, 412–425.

Hirata, R., Hirano, T., Saigusa, N., Fujinuma, Y., Inukai, K., Kitamori, Y., Takahashi, Y., Yamamoto, S., 2007. Seasonal and interannual variations in carbon dioxide exchange of a temperate larch forest. Agric. Forest Meteorol. 147, 110–124.

Howard, E.A., Gower, S.T., Foley, J.A., Kucharik, C.J., 2004. Effects of logging on carbon dynamics of a jack pine forest in Saskatchewan, Canada. Global Change Biol. 10, 1267–1284.

Humphreys, E.R., Black, T.A., Morgenstern, K., Cai, T., Drewitt, G.B., Nesic, Z., Trofymow, J.A., 2006. Carbon dioxide fluxes in coastal Douglas-fir stands at different stages of development after clearcut harvesting. Agric. Forest Meteorol. 140, 6–22.

Irvine, J., Law, B.E., Hibbard, K.A., 2007. Postfire carbon pools and fluxes in semiarid ponderosa pine in Central Oregon. Global Change Biol. 13, 1748–1760.

Jacobs, C.M.J., Jacobs, A.F.G., Bosveld, F.C., Hendriks, D.M.D., Hensen, A., Kroon, P.S., Moors, E.J., Nol, L., Schrier-Uijl, A., Veenendaal, E.M., 2007. Variability of annual CO_2 exchange from Dutch grasslands. Biogeosciences 4, 803–816.

Jenkins, J.P., Richardson, A.D., Braswell, B.H., Ollinger, S.V., Hollinger, D.Y., Smith, M.L., 2007. Refining light-use efficiency calculations for a deciduous forest canopy using simultaneous tower-based carbon flux and radiometric measurements. Agric. Forest Meteorol., 64–79.

Kato, T., Tang, Y., Gu, S., Hirota, M., Du, M., Li, Y., Zhao, X., 2006. Temperature and biomass influences on interannual changes in CO_2 exchange in an alpine meadow on the Qinghai-Tibetan Plateau. Global Change Biol. 12, 1285–1298.

Kattge, J., Knorr, W., 2007. Temperature acclimation in a biochemical model of photosynthesis: a reanalysis of data from 36 species. Plant Cell Environ. 30, 1176–1190.

Kleidon, A., Fraedrich, K., Low, C., 2007. Multiple steady-states in the terrestrial atmosphere-biosphere system: a result of a discrete vegetation classification? Biogeosciences 4, 707–714.

Knohl, A., Schulze, E.D., Kolle, O., Buchmann, N., 2003. Large carbon uptake by an unmanaged 250-year-old deciduous forest in Central Germany. Agric. Forest Meteorol. 118, 151–167.

Knorr, W., Kattge, J., 2005. Inversion of terrestrial ecosystem model parameter values against eddy covariance measurements by Monte Carlo sampling. Global Change Biol. 11, 1333–1351.

Krinner, G., Viovy, N., de Noblet-Ducoudré, N., Ogée, J., Polcher, J., Friedlingstein, P., Ciais, P., Sitch, S., Prentice, I.C., 2005. A dynamic global vegetation model for studies of the coupled atmosphere–biosphere system. Global Biogeochem. Cycles 19, GB1015.

Krishnan, P., Black, T.A., Barr, A.G., Grant, N.J., Gaumont-Guay, D., Nesic, Z., 2008. Factors controlling the interannual variability in the carbon balance of a southern boreal black spruce forest. J. Geophys Res. D: Atmos. 113, D09109.

Kull, O., Jarvis, P.G., 1995. The role of nitrogen in a simple scheme to scale up photosynthesis from leaf to canopy. Plant Cell Environ. 18, 1174–1182.

Lafleur, P.M., Roulet, N.T., Bubier, J.L., Frolking, S., Moore, T.R., 2003. Interannual variability in the peatland–atmosphere carbon dioxide exchange at an ombrotrophic bog. Global Biochem. Cycles 17, 1036.

Lagarias, J.C., Reeds, J.A., Wright, M.H., Wright, P.E., 1998. Convergence properties of the Nelder-Mead simplex method in low dimensions. SIAM J. Optim. 9, 122–147.

Lagergren, F., Lindroth, A., Dellwik, E., Ibrom, A., Lankreijer, H., Launiainen, S., Mölder, M., Kolari, P., Pilegaard, K., Vesala, T., 2008. Biophysical controls on CO_2 fluxes of three Northern forests based on long-term eddy covariance data. Tellus 60B, 143–152.

Lasslop, G., Reichstein, M., Kattge, J., Papale, D., 2008. Influences of observation errors in eddy flux data on inverse model parameter estimation. Biogeosciences 5, 1311–1324.

Law, B.E., Falge, E., Gu, L., Baldocchi, D.D., Bakwin, P., Berbigier, P., Davis, K., Dolman, A.J., Falk, M., Fuentes, J.D., Goldstein, A., Granier, A., Grelle, A., Hollinger, D., Janssens, I.A., Jarvis, P., Jensen, N.O., Katul, G., Mahli, Y., Matteucci, G., Meyers, T., Monson, R., Munger, W., Oechel, W., Olson, R., Paw U, K.T., Pilegaard, K., Thorgeirsson, H., Valentini, R., Verma, S., Vesala, T., Wilson, K., Wofsy, S., 2002. Environmental controls over carbon dioxide and water vapor exchange of terrestrial vegetation. Agric. Forest Meteorol. 113, 97–120.

Leuning, R., 1995. A critical appraisal of a combined stomatal-photosynthesis model for C_3 plants. Plant Cell Environ. 18, 339–355.

Leuning, R., 2002. Temperature dependence of two parameters in a photosynthesis model. Plant Cell Environ. 25, 1205–1210.

Liu, H., Randerson, J.T., Lindfors, J., Chapin III, F.S., 2005. Changes in the surface energy budget after fire in boreal ecosystems of interior Alaska: an annual perspective. J. Geophys Res. D: Atmos. 110, 13101.

Lund, M., Lindroth, A., Christensen, T., 2007. Annual CO_2 balance of a temperate bog. Tellus 59B, 804–811.

Luyssaert, S., Inglima, I., Jung, M., Richardson, A.D., Reichstein, M., Papale, D., Piao, S.L., Schulze, E.D., Wingate, L., Matteucci, G., Aragao, L., Aubinet, M., Beer, C., Bernhofer, C., Black, K.G., Bonal, D., Bonnefond, J.M., Chambers, J., Ciais, P., Cook, B., Davis, K.J., Dolman, A.J., Gielen, B., Goulden, M., Grace, J., Granier, A., Grelle, A., Griffis, T., Grünwald, T., Guidolotti, G., Hanson, P.J., Harding, R., Hollinger, D.Y., Hutyra, L.R., Kolari, P., Kruijt, B., Kutsch, W., Lagergren, F., Laurila, T., Law, B.E., Le Mair, G., Lindroth, A., Loustau, D., Malhi, Y., Mateus, J., Migliavacca, M., Misson, L., Montagnani, L., Moncrieff, J., Moors, E., Munger, J.W., Nikinmaa, E., Ollinger, S.V., Pita, G., Rebmann, C., Roupsard, O., Saigusa, N., Sanz, M.J., Seufert, G., Sierra, C., Smith, M.L., Tang, J., Valentini, R., Vesala, T., Janssens, I.A., 2007. CO_2 balance of boreal, temperate, and tropical forests derived from a global database. Global Change Biol. 13, 2509–2537.

Marcolla, B., Pitacco, A., Cescatti, A., 2003. Canopy architecture and turbulence structure in a coniferous forest. Boundary-Layer Meteorol. 108, 39–59.

Matsumoto, K., Ohta, T., Nakai, T., Kuwada, T., Daikoku, K., Iida, S., Yabuki, H., Kononov, A.V., van der Molen, M.K., Kodama, Y., Maximov, T.C., Dolman, A.J., Hattori, S., 2008. Responses of surface conductance to forest environments in the Far East. Agric. Forest Meteorol. 148, 1926–1940.

Medlyn, B.E., Dreyer, E., Ellsworth, D., Forstrueter, M., Harley, P.C., Kirschbaum, M.U.F., Le Roux, X., Montpied, P., Strassemeyer, J., Walcroft, A., Wang, K., Loustau, D., 2002a. Temperature response of parameters of a biochemically based

model of photosynthesis. II. A review of experimental data. Plant Cell Environ. 25, 1167–1179.
Medlyn, B.E., Loustau, D., Delzon, S., 2002b. Temperature response of parameters of a biochemically based model of photosynthesis. I. Seasonal changes in mature maritime pine (Pinus pinaster. Ait.). Plant Cell Environ. 25b, 1155–1165.
Meinzer, F.C., 2003. Functional convergence in plant responses to the environment. Oecologia 134, 1–11.
Mercado, L.M., Lloyd, J., Dolman, A.J., Sitch, S., Patino, S., 2009. Modelling basin-wide variations in Amazon forest productivity – Part 1: Model calibration, evaluation and upscaling functions for canopy photosynthesis. Biogeosciences 6, 1247–1272.
Misson, L., Tang, J., Xu, M., McKay, M., Goldstein, A., 2005. Influences of recovery from clear-cut, climate variability, and thinning on the carbon balance of a young ponderosa pine plantation. Agric. Forest Meteorol. 130, 207–222.
Mkhabela, M.S., Amiro, B.D., Barr, A.G., Black, T.A., Hawthorne, I., Kidston, J., McCaughey, J.H., Orchansky, A.L., Nesic, Z., Sass, A., Shashkov, A., Zha, T., 2009. Comparison of carbon dynamics and water use efficiency following fire and harvesting in Canadian boreal forests. Agric. Forest Meteorol. 149, 783–794.
Moffat, A.M., Papale, D., Reichstein, M., Hollinger, D.Y., Richardson, A.D., Barr, A.G., Beckstein, C., Braswell, B.H., Churkina, G., Desai, A.R., Falge, E., Gove, J.H., Heimann, M., Hui, D., Jarvis, A.J., Kattge, J., Noormets, A., Stauch, V.J., 2007. Comprehensive comparison of gap-filling techniques for eddy covariance net carbon fluxes. Agric. Forest Meteorol. 147, 209–232.
Monson, R.K., Turnipseed, A.A., Sparks, J.P., Harley, P.C., Scott-Denton, L.E., Sparks, K., Huxman, T.E., 2002. Carbon sequestration in a high-elevation, subalpine forest. Global Change Biol. 8, 459–478.
Montagnani, L., Manca, G., Canepa, E., Georgieva, E., Acosta, M., Feigenwinter, C., Janous, D., Kerschbaumer, G., Lindroth, A., Minach, L., Minerbi, S., Mölder, M., Pavelka, M., Seufert, G., Zeri, M., Ziegler, W., 2009. A new mass conservation approach to the study of CO_2 advection in an alpine forest. J. Geophys Res. D: Atmos. 114, 07306.
Noormets, A., Chen, J., Crow, T.R., 2007. Age-dependent changes in ecosystem carbon fluxes in managed forests in Northern Wisconsin, USA. Ecosystems, 10.
Noormets, A., Gavazzi, M.J., McNulty, S.G., Domec, J.C., Sun, G., King, J.S., Chen, J., 2010. Response of carbon fluxes to drought in a coastal plain loblolly pine forest. Global Change Biol. 16, 272–287.
ORNL DAAC, 2009. MODIS subsetted land products. Collection 5. Available online http://www.daac.ornl.gov/MODIS/modis.html from ORNL DAAC, Oak Ridge, Tennessee, U.S.A.
Owen, K.E., Tenhunen, J., Reichstein, M., Wang, Q., Falge, E., Geyer, R., Xiao, X., Stoy, P., Amman, C., Afrain, A., Aubinet, M., Aurela, M., Bernhofer, C., Chojnicki, B.H., Granier, A., Gruenwald, T., Hadley, J., Heinesch, B., Hollinger, D., Knohl, A., Kutsch, W., Lohila, A., Meyers, T., Moors, E., Moureaux, C., Pilegaard, K., Saigusa, N., Verma, S., Vesala, T., Vogel, C., 2007. Linking flux network measurements to continental scale simulations: ecosystem carbon dioxide exchange capacity under non-water-stressed conditions. Global Change Biol. 13, 1–27.
Papale, D., Reichstein, M., Aubinet, M., Canfora, E., Bernhofer, C., Kutsch, W., Longdoz, B., Rambal, S., Valentini, R., Vesala, T., Yakir, D., 2006. Towards a standardized processing of net ecosystem exchange measured with eddy covariance technique: algorithms and uncertainty estimation. Biogeosciences 3, 571–583.
Papale, D., Valentini, R., 2003. A new asssesment of European forests carbon exchanges by eddy fluxes and artificial neural network spatialization. Global Change Biol. 9, 525–535.
Pataki, D.E., Oren, R., 2003. Species differences in stomatal control of water loss at the canopy scale in a mature bottomland deciduous forest. Adv. Water Resour. 26, 1267–1278.
Pilegaard, K., Mikkelsen, T.N., Beier, C., Jensen, N.O., Ambus, P., Ro-Poulsen, H., 2003. Field measurements of atmosphere–biosphere interactions in a Danish beech forest. Bor. Environ. Res. 8, 315–333.
Pintér, K., Barcza, Z., Balogh, J., Czóbel, S., Csintalan, Z., Tuba, Z., Nagy, Z., 2008. Interannual variability of grasslands' carbon balance depends on soil type. Commun. Ecol. 9, 43–48.
Pitman, A.J., 2003. The evolution of, and revolution in, land surface schemes designed for climate models. Int. J. Clim. 23, 479–510.
Powell, T.L., Bracho, R., Li, J., Dore, S., Hinkle, C.R., Drake, B.G., 2006. Environmental controls over net ecosystem carbon exchange of scrub oak in central Florida. Agric. Forest Meteorol. 141, 19–34.
Raupach, M.R., Rayner, P.J., Barrett, D.J., Defries, R.S., Heimann, M., Ojima, D.S., Quegan, S., Schmullius, C.C., 2005. Model-data synthesis in terrestrial carbon observations: methods, data requirements and data uncertainty specifications. Global Change Biol. 11, 378–397.
Rayner, P.J., Scholze, M., Knorr, W., Kaminski, T., Giering, R., Widmann, H., 2005. Two decades of terrestrial carbon fluxes from a carbon cycle data assimilation system (CCDAS). Global Biogeochem. Cycles 19, GB2026.
Rebmann, C., Göckede, M., Foken, T., Aubinet, M., Aurela, M., Berbigier, P., Bernhofer, C., Buchmann, N., Carrara, A., Cescatti, A., Ceulemans, R., Clement, R., Elbers, J.A., Granier, A., Grünwald, T., Guyon, D., Havránková, K., Heinesch, B., Knohl, A., Laurila, T., Longdoz, B., Marcolla, B., Markkanen, T., Miglietta, F., Moncrieff, J., Montagnani, L., Moors, E., Nardino, M., Ourcival, J.M., Rambal, S., Rannik, U., Rotenberg, E., Sedlak, P., Unterhuber, G., Vesala, T., Yakir, D., 2005. Quality analysis applied on eddy covariance measurements at complex forest sites using footprint modelling. Theor. Appl. Climatol., 80.
Rebmann, C., Zeri, M., Lasslop, G., Mund, M., Kolle, O., Schulze, E.D., Feigenwinter, C., 2010. Treatment and assessment of the CO_2-exchange at a complex forest site in Thuringia, Germany. Agric. Forest Meteorol. 150, 684–691.
Reich, P.B., Walters, M.B., Ellsworth, D.S., 1997. From tropics to tundra: Global convergence in plant functioning. Proc. Nat. Acad. Sci. U.S.A. 94, 13730–13734.
Reichstein, M., Falge, E., Baldocchi, D., Papale, D., Aubinet, M., Berbignier, P., Bernhofer, C., Buchmann, N., Gilmanov, T., Granier, A., Grunwald, T., Havranovka, K., Ilvesniemi, H., Janous, D., Knohl, A., Laurila, T., Lohila, A., Loustau, D., Mattuecci, G., Meyers, T., Miglietta, F., Ourcival, J.M., Pumpanen, J., Rambal, S., Rotenberg, E., Sanz, M., Tenhunen, J., Seufert, G., Vaccari, F., Vesala, T., Yakir, D., Valentini, R., 2005. On the separation of net ecosystem exchange into assimilation and ecosystem respiration: review and improved algorithm. Global Change Biol. 11, 1424–1439.
Reichstein, M., Rey, A., Freibauer, A., Tenhunen, J., Valentini, R., Banza, J., Casals, P., Cheng, Y., Grünzweig, J.M., Irvine, J., Joffre, R., Law, B.E., Loustau, D., Miglietta, F., Oechel, W., Ourcival, J.M., Pereira, J.S., Peressotti, A., Ponti, F., Qi, Y., Rambal, S., Rayment, M., Romanya, J., Rossi, F., Tedeschi, V., Tirone, G., Xu, M., Yakir, D., 2003a. Modeling temporal and large-scale spatial variability of soil respiration from soil water availability, temperature and vegetation productivity indices. Global Biochem. Cycles 17, 1104.
Reichstein, M., Tenhunen, J., Roupsard, O., Ourcival, J.M., Rambal, S., Miglietta, F., Peressotti, A., Pecchiari, M., Tirone, G., Valentini, R., 2003b. Inverse modeling of seasonal drought effects on canopy CO_2/H_2O exchange in three Mediterranean ecosystems. J. Geophys Res. D: Atmos. 108, 4726.
Rey, A., Pegoraro, E., Tedeschi, V., De Parri, I., Jarvis, P.G., Valentini, R., 2002. Annual variation in soil respiration and its components in a coppice oak forest in Central Italy. Global Change Biol. 8, 851–866.
Richardson, A.D., Hollinger, D.Y., 2005. Statistical modeling of ecosystem respiration using eddy covariance data: maximum likelihood parameter estimation, and Monte Carlo simulation of model and parameter uncertainty, applied to three simple models. Agric. Forest Meteorol. 131, 191–208.
Richardson, A.D., Hollinger, D.Y., Aber, J.D., Ollinger, S.V., Braswell, B.H., 2007. Environmental variation is directly responsible for short- but not long-term variation in forest–atmosphere carbon exchange. Global Change Biol. 13, 788–803.
Richardson, A.D., Hollinger, D.Y., Burba, G.G., Davis, K.J., Flanagan, L.B., Katul, G.G., Munger, J.W., Ricciuto, D.M., Stoy, P.C., Suyker, A.E., Verma, S.B., Wofsy, S.C., 2006. A multi-site analysis of random error in tower-based measurements of carbon and energy fluxes. Agric. Forest Meteorol. 136, 1–18.
Richardson, A.D., Mahecha, M.D., Falge, E., Kattge, J., Moffat, A.M., Papale, D., Reichstein, M., Stauch, V.J., Braswell, B.H., Churkina, G., Kruijt, B., Hollinger, D.Y., 2008. Statistical properties of random CO_2 flux measurment uncertainty inferred from model residuals. Agric. Forest Meteorol. 148, 38–50.
Roupsard, O., Bonnefond, J.M., Irvine, M., Berbigier, P., Nouvellon, Y., Dauzat, J., Taga, S., Hamel, O., Jourdan, C., Saint-Andrè, L., Mialet-Serra, I., Labouisse, J.P., Epron, D., Joffre, R., Braconnier, S., Rouzière, A., Navarro, M., Bouillet, J.P., 2006. Partitioning energy and evapo-transpiration above and below a tropical palm canopy. Agric. Forest Meteorol. 139, 252–268.
Santos, A.J.B., Quesada, C.A., Da Silva, G.T., Maia, J.F., Miranda, H.S., Miranda, A.C., Lloyd, J., 2004. High rates of net ecosystem carbon assimilation by Brachiara pasture in the Brazilian Cerrado. Global Change Biol. 10, 877–885.
Sanz, M.J., Carrara, A., Gimeno, C., 2004. Effects of a dry and warm summer conditions on CO_2 and energy fluxes from three Meditteranean ecosystems. Geophys. Res. Abst. 6, 3239.
Schmid, H.P., Grimmond, C.S.B., Cropley, F., Offerle, B., Su, H.B., 2000. Measurements of CO_2 and energy fluxes over a mixed hardwood forest in the mid-western United States. Agric. Forest Meteorol. 103, 357–374.
Schymanski, S.J., Roderick, M.L., Sivapalan, M., Hutley, L.B., Beringer, J., 2007. A canopy-scale test of the optimal water-use hypothesis. Plant Cell Environ. 31, 97–111.
Schymanski, S.J., Sivapalan, M., Roderick, M.L., Hutley, L.B., Beringer, J., 2009. An optimality-based model of the dynamic feedbacks between natural vegetation and the water balance. Water Resour. Res. 45, W01412.
Seber, G.A.F., 1984. Multivariate Observations. Wiley, New York.
Sellers, P.J., Berry, J.A., Collatz, G.J., Field, C.B., Hall, F.G., 1992. Canopy reflectance, photosynthesis and transpiration. III. A reanalysis using improved leaf models and a new canopy integration scheme. Remote Sens. Environ. 42, 187–216.
Sellers, P.J., Dickinson, R.E., Randall, D.A., Betts, A.K., Hall, F.G., Berry, J.A., Collatz, G.J., Denning, A.S., Mooney, H.A., Nobre, C.A., Sato, N., Field, C.B., Henderson-Sellers, A., 1997. Modeling the exchanges of energy, water, and carbon between continents and the atmosphere. Science 275, 502–509.
Sellers, P.J., Mintz, Y., Sud, Y., Dalcher, A., 1986. A simple biosphere model (SiB) for use within general circulation models. J. Atmos. Sci. 43, 505–531.
Sellers, P.J., Randall, D.A., Collatz, G.J., Berry, J.A., Field, C.B., Dazlich, D.A., Zhang, C., Collelo, G.D., Bounoua, L., 1996. A revised land surface parametererization (SiB2) for atmospheric GCMs. Part I: Model formulation. J. Clim. 9, 676–705.
Sitch, S., Smith, B., Prentice, I.C., Arneth, A., Bondeau, A., Cramer, W., Kaplan, J.O., Levis, S., Lucht, W., Sykes, M.T., Thonicke, K., Venevsky, S., 2003. Evaluation of ecosystem dynamics, plant geography and terrestrial carbon cycling in the LPJ dynamic global vegetation model. Global Change Biol. 9, 161–185.
Stöckli, R., Lawrence, D.M., Niu, G.Y., Oleson, K.W., Thornton, P.E., Yang, Z.L., Bonan, G.B., Denning, A.S., Running, S.W., 2008. Use of FLUXNET in the Community Land Model development. J. Geophys Res. G: Biogeosci. 113, 01025.
Stoy, P.C., Richardson, A.D., Baldocchi, D.D., Katul, G.G., Stanovick, J., Mahecha, M.D., Reichstein, M., Detto, M., Law, B.E., Wohlfahrt, G., Arriga, N., Campos, J., McCaughey, J.H., Montagnani, L., Paw U., K.T., Sevanto, S., Williams, M., 2009. Biosphere–atmosphere exchange of CO_2 in relation to climate: a cross-biome analysis across multiple time scales. Biogeosciences 6, 2297–2312.
Suni, T., Berninger, F., Vesala, T., Markkanen, T., Hari, P., Mäkelä, A., Ilvesniem, H., Hänninen, H., Nikinmaa, E., Huttula, T., Laurila, T., Aurela, M., Grelle, A., Lindroth,

A., Arneth, A., Shibistova, O., Lloyd, J., 2003a. Air temperature triggers the recovery of evergreen boreal forest photosynthesis in spring. Global Change Biol. 9, 1410–1426.

Suni, T., Rinne, J., Reissell, A., Altimir, N., Keronen, P., Rannik, Ü., Maso, M.D., Kulmala, M., Vesala, T., 2003b. Long-term measurements of surface fluxes above a Scots pine forest in Hyytiälä, southern Finland, 1996–2001. Bor. Environ. Res. 8, 287–301.

Thornton, P.E., Doney, S.C., Lindsay, K., Moore, J.K., Mahowald, N., Randerson, J.T., Fung, I., Lamarque, J.F., Feddema, J.J., Lee, Y.H., 2009. Carbon–nitrogen interactions regulate climate–carbon cycle feedbacks: results from an atmosphere–ocean general circulation model. Biogeosciences 6, 2099–2120.

Thum, T., Aalto, T., Laurila, T., Aurela, M., Lindroth, A., Vesala, T., 2008. Asessing seasonality of seasonality of biochemical CO_2 exhange model parameters from micrometeorological flux observations at boreal coniferous forest. Biogeosciences 5, 1625–1639.

van der Tol, C., Dolman, A.J., Waterloo, M.J., Raspor, K., 2007. Topography induced spatial variations in diurnal cycles of assimilation and latent heat of mediterranean forest. Biogeosciences 4, 137–154.

van der Tol, C., Meesters, A.G.C.A., Dolman, A.J., Waterloo, M.J., 2008. Optimum vegetation characteristics, assimilation, and transpiration during a dry season: 1. Model description. Water Resour. Res. 44, W03421+.

van Dijk, A.J., Dolman, A.J., 2004. Estimates of CO_2 uptake and release among European forests based on eddy covariance data. Global Change Biol. 10, 1445–1459.

Valentini, R., Angelis, P.D., Matteuci, G., Monaco, R., Dore, S., Scarascia Mucnozza, G.E., 1996. Seasonal net carbon dioxide exchange of a beech forest with the atmosphere. Global Change Biol. 2, 199–207.

Verbeeck, H., Samson, R., Granier, A., Montpied, P., Lemeur, R., 2008. Multi-year model analysis of GPP in a temperate beech forest in France. Ecol. Model. 210, 85–103.

von Caemmerer, S., Farquhar, G.D., 1981. Some relationships between the biochemistry of photosynthesis and the gas exchange of leaves. Planta 153, 376–387.

Vickers, D., Thomas, C., Law, B.E., 2009. Random and systematic CO_2 flux sampling errors for tower measurements over forests in the convective boundary layer. Agric. Forest Meteorol. 149, 73–83.

Wang, A., Price, D.T., 2007. Estimating global distribution of boreal, temperate, and tropical tree plant functional types using clustering techniques. J. Geophys Res. G: Biogeosci. 112, G01024.

Wang, Y.P., Baldocchi, D., Leuning, R., Falge, E., Vesala, T., 2007. Estimating parameters in a land-surface model by applying nonlinear inversion to eddy covariance flux measurements from eight FLUXNET sites. Global Change Biol. 12, 1–19.

Williams, M., Richardson, A.D., Reichstein, M., Stoy, P.C., Peylin, P., Verbeeck, H., Carvalhais, N., Jung, M., Hollinger, D.Y., Kattge, J., Leuning, R., Luo, Y., Tomelleri, E., Trudinger, C.M., Wang, Y.P., 2009. Improving land surface models with FLUXNET data. Biogeosciences 6, 1341–1359.

Wohlfahrt, G., Hammerle, A., Haslwanter, A., Bahn, M., Tappeiner, U., Cernusca, A., 2008. Seasonal and inter-annual variability of the net ecosystem CO_2 exchange of a temperate mountain grassland: effects of weather and management. J. Geophys Res. D: Atmos. 113, D08110.

Wolf, A., Ashalov, K., Saliendra, N., Johnson, D.A., Laca, E.A., 2006. Inverse estimation of Vc_{max}, leaf area index, and the Ball-Berry parameter from carbon and energy fluxes. J. Geophys Res. D: Atmos. 111, D08S08.

Wood, S.A., Beringer, J., Hutley, L.B., McGuire, A.D., van Dijk, A.J., Kilinc, M., 2008. Impacts of fire on forest age and runoff in mountain ash forests. Funct. Plant Biol. 35, 483–492.

Woodward, F.I., Cramer, W., 1996. Plant functional types and climatic changes: introduction. J. Veg. Sci. 7, 306–308.

Woodward, F.I., Lomas, M.R., Betts, R.A., 1998. Vegetation-climate feedbacks in a greenhouse world. Philos. Trans. R. Soc. Lond., Ser. B 353, 29–39.

Wright, I.J., Reich, P.B., Westoby, M., Ackerly, D.D., Baruch, Z., Bongers, F., Cavendar-Bares, J., Chapin, T., Cornelissen, J.H.C., Diemer, M., Flexas, J., Garnier, E., Groom, P.K., Gulias, J., Hikosaka, K., Lamont, B., Lee, T., Lee, W., Lusk, C., Midgley, J.J., Navas, M.L., Niinemets, Ü., Oleksyn, J., Osada, N., Poorter, H., Poot, P., Prior, L., Pyankov, V.I., Roumet, C., Thomas, S.C., Tjoelker, M., Veneklaas, E., Villar, R., 2004. The worldwide leaf economics spectrum. Nature 428, 821–827.

Yan, Y., Zhao, B., Chen, J., Guo, H., Gu, Y., Wu, Q., Li, B., 2008. Closing the carbon budget of estuarine wetlands with tower-based measurements and MODIS time series. Global Change Biol. 14, 1690–1702.

Yang, X., Wittig, V., Jain, A.K., Post, W., 2009. Integration of nitrogen cycle dynamics into the Integrated Science Assessment Model for the study of terrestrial ecosystem responses to global change. Global Biogeochem. Cycles 23, GB4029.

Yuan, W., Luo, Y., Richardson, A.D., Oren, R., Luyssaert, S., Janssens, I.A., Ceulemans, R., Zhou, X., Grünwald, T., Aubinet, M., Berhofer, C., Baldocchi, D.D., Chen, J., Dunn, A.L., Deforest, J.L., Dragoni, D., Goldstein, A.H., Moors, E., Munger, J.W., Monson, R.K., Suyker, A.E., Starr, G., Scott, R., Tenhunen, J., Verma, S.B., Vesala, T., Wofsy, S.C., 2009. Latitudinal patterns of magnitude and interannual variability in net ecosystem exchange regulated by biological and environmental variables. Global Change Biol. 15, 2905–2920.

Zaehle, S., Friend, A.D., 2010. Carbon and nitrogen cycle dynamics in the O–CN land surface model: 1. Model description, site-scale evaluation, and sensitivity to parameter estimates. Global Biogeochem. Cycles 24, GB1005.

Zha, T., Barr, A.G., Black, T.A., McCaughey, J.H., Bhatti, J., Hawthorne, I., Krishnan, P., Kidston, J., Saigusa, N., Shashkov, A., Nesic, Z., 2009. Carbon sequestration in boreal jack pine stands following harvesting. Global Change Biol. 15, 1475–1487.